A BGK-type Flux-vector Splitting Scheme for the Ultra-relativistic Euler Equations *

Matthias Kunik[†], Shamsul Qamar[‡] and Gerald Warnecke[§]
Institute for Analysis and Numerics, Otto-von-Guericke University
PSF 4120. D-39106 Magdeburg, Germany

January 9, 2003

Abstract. A gas-kinetic solver is developed for the ultra-relativistic Euler equations. The scheme is based on the direct splitting of the flux function of the Euler equations with inclusion of "particle" collisions in the transport process. Consequently, the artificial dissipation in the new scheme is much reduced in comparison with the usual kinetic flux vector splitting (KFVS) schemes which are based on the free particle transport at the cell interfaces in the gas evolution stage. Although in a usual KFVS scheme the free particle transport gives robust solution, it gives smeared solution at the contact discontinuities. The new BGK-type KFVS scheme solves this problem and gives robust and reliable solutions as well as good resolution at the contact discontinuity. The scheme is naturally multidimensional and is extended to the two-dimensional case in a usual dimensionally split manner, that is, the formulae for the fluxes can be used along each coordinate direction. The high-order resolution of the scheme is achieved by using MUSCL-type initial reconstruction. In the numerical case studies the results obtained from the BGK-type KFVS schemes are compared with the exact solution, KFVS schemes, upwind schemes and central schemes.

Key words: hyperbolic systems, ultra-relativistic Euler equations, BGK-type KFVS scheme, numerical dissipation, higher order accuracy.

Subject classification: 65M99, 65Y20.

*This work is supported by the DFG Priority Research Program project "Kinetic methods for selected initial and boundary value problems."

[†]matthias.kunik@mathematik.uni-magdeburg.de
[‡]shamsul.qamar@mathematik.uni-magdeburg.de
[§]gerald.warnecke@mathematik.uni-magdeburg.de

1 Introduction

In recent years relativistic gas dynamics plays an important role in areas of astrophysics, high energy particle beams, high energy nuclear collisions, and free-electron laser technology. The equations that describe the relativistic gas dynamics are highly nonlinear. Several numerical methods for solving relativistic gas dynamics have been reported. All these methods are mostly developed from the existing reliable methods for solving the Euler equations of nonrelativistic or Newtonian gas dynamics, see Martí and Müller [22] and references therein.

Kunik, Qamar and Warnecke [16, 17] have used for the first time kinetic schemes in order to solve the relativistic Euler equations. They combined the already developed physical framework of the relativistic kinetic theory of gases with mathematical and numerical analysis of the relativistic Euelr equations, see deGroot [11].

In the past decades, tremendous progress has been made in the development of numerical methods for compressible flow simulations. Most of them are largely based on the upwind concepts, see [10, 12, 23]. There are mainly two kinds of flux functions derived from the inviscid Euler equations. The first group is the flux vector splitting (FVS) schemes. Flux splitting is a technique for achieving upwinding bias in numerical flux function, which is a natural consequence of regarding a fluid as an ensemble of particles. Since particles can move forward or backward, this automatically splits the fluxes of mass, momentum and energy into forward and backward fluxes through the cell interface, i.e.,

$$F_{i+\frac{1}{2}} = F^+(W_i) + F^-(W_{i+1}),$$

where W_i represents mass, momentum and energy densities inside the cell i. The equivalence between the above splitting mechanism and the collisionless Boltzmann equation was first realized by Harten, Lax and van Leer [12]. Numerically it is observed that the explicit flux formulation of the KFVS schemes by solving collisionless Boltzmann equation is identical to the flux function of van Leer [21]. We will discuss the KFVS scheme for the solution of ultra-relativistic Euler equations. For more discussion on the KFVS schemes the reader is refered to Xu et. al [35] and Xu [36, 37, 38].

On the other hand, the FDS schemes based on the exact or approximate Riemann solvers, such as the Godunov, Roe and Osher methods [9, 24, 28], account for the wave interactions in the gas evolution process. Especially for the Godunov method, the exact solution of the Euler equations is used. The wave interaction in the FDS scheme can be clearly observed in the Roe's average $\overline{W}_{i+\frac{1}{2}}$ between the left W_i and the right state W_{i+1}. In the smooth flow region, there is basically no differences among the Godunov, Roe and Osher schemes. For example, the above three schemes can precisely keep a shear layer in the 2D case once the shear layer is aligned with the mesh. This fact is consistent with the exact solution of the

Euler equations. Therefore, the FDS schemes can accuratly capture the Navier-Stokes solutions in the resolved dissipative boundary layer, where the numerical dissipation is much smaller than the physical dissipation, see Xu [38] for details. However, this advantage is also accompanied with a disadvantage, the Godunov scheme in strong shock regions produce spurious oscillations such as carbuncle phenomena and odd-even decoupling in multi-dimnsional case. FVS schemes do not generate these spurious solutions, since they are intrinsically solving "viscous" equations rather than the inviscid Euler equations. An optimum choice to get a better scheme is to combine both, the FVS and FDS methodology. This is the main aim of this paper using under consideration the ultra-relativistic case of the Euler equations.

Even with initial equilibrium states, the collisionless Boltzmann transport equation cannot keep the local equilibrium property dynamically. Physically, the mechanism for bringing the distribution function close to equilibrium state simulates the collisions suffered by the molecules of the gas, the so called collision term in the Boltzmann equation. But the collisionless Boltzmann equation in the free-transport evolution stage totally ignores the dynamical process of particle collisions.

Although the KFVS scheme lacks particle collisions in the free-transport evolution stage, numerically it still can be used in the compressible flow calculations, and the numerical solution is different from the free particle stream solutions. The basic reason for this is that an artificial collision term has been implicitly added in the projection stage. For example at the end of each time step, a Maxwellian distribution function f_M inside each cell is re-initiated, which is equivalent to perform particle collisions instantaneously to make the transition from non-equilibrium state, i.e. free-flight f, to equilibrium state f_M inside each cell. The dynamical effect from the two numerical stages (i.e. free-flight and projection) in the KFVS scheme is qualitatively discribed in the Figure 1, where the free transport in the gas evolution stage evolves the system away from the Euler solution (f becomes more and more different from a Maxwellian), the projection stage drives the system towards to the Euler solution (the instantaneous preparation of equilibrium states), see Xu [38].

Kinetic flux vector splitting schemes (KFVS) have been widely used in solving multidimensional classical Euler equations. Mandal and Despande [21] have applied KFVS to solve the bump in a channel problem with structured meshes. Weatherill *et al.* [33] have applied first order and high order KFVS schemes to several two-dimensional problems with structured and unstructured meshes. Deshpande *et al.* [4] have developed the three-dimensional time marching Euler code called BHEEMA using KFVS method for the aerodynamic design and analysis of practical configurations. Perthame [25] used kinetic flux splitting scheme to derive a second order KFVS scheme with the Maxwellian phase density which is second order accurate in time. This second order in time phase density was first obtained by Despande [3] to get second order kinetic scheme and is based on Chapman Enskog analy-

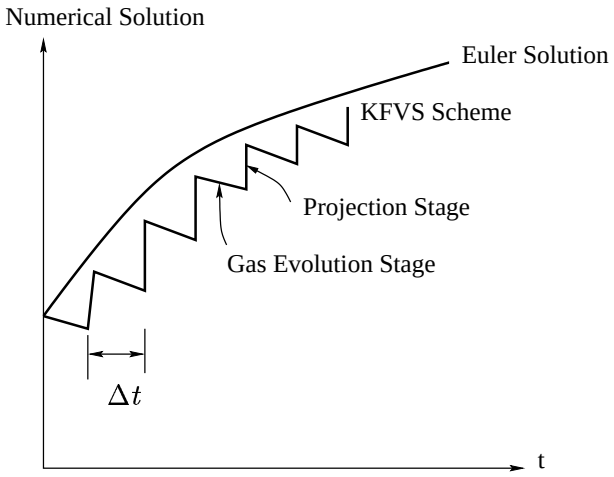

Figure 1: KFVS solution vs Euler solution, where Δt is a CFL time step.

sis for the solution of Boltzmann equation. Tang and Xu [30] proved the positivity of the KFVS based collisional Boltzmann scheme (BGK scheme) for the classical Euler equations, while Lui and Xu [20] proved the entropy inequality for this KFVS based BGK scheme. Deshpande and Kulkarni [5] also applied the idea of KFVS scheme on moving grids for the classical Euler equations.

The kinetic schemes developed in [16, 17] are discrete in time but continuous in space, and thus are unconditionally stable. The initial data in these schemes are the primitive field variables for the particle density n, the transformed velocity $\mathbf{u} = \mathbf{v}/\sqrt{1 - \frac{\mathbf{v}^2}{c^2}}$ and the temperature T. To get the values of the field variables at next time step in the free flight they use the algebraic combinations of the free-flight moments integrals, while to get field variables at each maximization time they use continuity conditions which are obtained from the constitutive relations for the Euler equations. These continuity conditions also guarantee the conservation laws for mass, momentum and energy.

In this paper we are interested to derive a new BGK-type KFVS scheme in order to solve ultra-relativistic Euler equations. In this new scheme the particle collisons are added to the free particle transport mechanism in the following convex combination form of the fluxes,

$$F_{i+\frac{1}{2}} = \eta F^f_{i+\frac{1}{2}} + (1-\eta) F^e_{i+\frac{1}{2}} \,,$$

where F^f is the flux term from the free flight phase density and F^e is equilibrium flux obtained from the equilibrium phase density which is relativistic Maxwellian (Jüttner phase density) in our case. Here η is an adjustable parameter and will be analyzed in the comming sections when we derive the scheme. These schemes have been sucessfully applied to the classical magnetohydrodynamics by Xu [37].

In the BGK-type KFVS scheme we start with a cell averaged initial data of the conservative variables and get back the cell averaged values of the conservative variables at the next time step. The scheme is multidimensional and will be extended to the two-dimensional case. In two-dimensional case the flux splitting is done in a usual dimensionally split manner, that is, the formulae for the fluxes can be used along each coordinate direction. In order to get second order accuracy we use the MUSCL-type reconstruction in both one and two-dimensional cases.

In order to formulate the theory in a Lorentz-invariant form, we make use of the notations for the tensor calculus used in the textbook of Weinberg [34], with only slight modifications:

A) **The space-time coordinates** are x^μ, $\mu = 0, 1, 2, 3$, with $x^0 := ct$ for the time, x^1, x^2, x^3 for the position.

B) **The metric-tensor** is

$$g_{\mu\nu} = g^{\mu\nu} = \begin{cases} +1 & , \quad \mu = \nu = 0\,, \\ -1 & , \quad \mu = \nu = 1, 2, 3\,, \\ 0 & , \quad \mu \neq \nu\,. \end{cases} \tag{1.1}$$

C) **The proper Lorentz-transformations** are linear transformations $\Lambda^\alpha_{\ \beta}$ from one system of space-time with coordinates x^α to another system x'^α. They must satisfy

$$x'^\alpha = \Lambda^\alpha_{\ \beta}\, x^\beta,\ g_{\mu\nu} = \Lambda^\alpha_{\ \mu}\, \Lambda^\beta_{\ \nu}\, g_{\alpha\beta},\ \Lambda^0_{\ 0} \geq 1,\ \det \Lambda = +1\,. \tag{1.2}$$

The conditions $\Lambda^0_{\ 0} \geq 1$ and $\det \Lambda = +1$ are necessary in order to exclude inversion in time and space. Then the following quantity forms a tensor with respect to proper Lorentz-transformations, the so called Levi-Civita tensor:

$$\epsilon_{\alpha\beta\gamma\delta} = \begin{cases} +1, & \alpha\beta\gamma\delta \text{ even permutation of } 0123, \\ -1, & \alpha\beta\gamma\delta \text{ odd permuation of } 0123\,, \\ 0, & \text{otherwise.} \end{cases}$$

Note that in the textbook of Weinberg [34] this tensor as well as the metric tensor both take the sign opposite to the notation used here.

D) **Einstein's summation convention:**
Any Greek index like α, β, that appears twice, once as a subscript and once as a superscript, is understood to be summed over 0,1,2,3 if not noted otherwise. For spatial indices, which are denoted by Latin indices like i, j, k, we will not apply this summation convention.

Now we take a microscopic look at the gas and start with the kinematics of a representative gas atom with particle trajectory $\mathbf{x} = \mathbf{x}(t)$, where the time coordinate t and the space coordinate $\mathbf{x}$ are related to an arbitrary Lorentz-frame. The invariant mass of all structureless particles is assumed to be the same and is denoted by m_0. The microscopic velocity of the gas atom is $\frac{d\,\mathbf{x}(t)}{dt}$, and its microscopic velocity four-vector is given by $c\,q^\mu$, where the *dimensionless microscopic velocity four-vector* q^μ is defined by

$$\left(q^0, \mathbf{q}\right)^T, \qquad q^0 = q_0 = \sqrt{1+\mathbf{q}^2}, \qquad \mathbf{q} = \frac{\frac{1}{c}\frac{d\mathbf{x}}{dt}}{\sqrt{1-\left(\frac{1}{c}\frac{d\mathbf{x}}{dt}\right)^2}}. \tag{1.4}$$

Note that in the ultra relativistic case $q^0 = |\mathbf{q}|$, see [16, 17] for further details.

The *relativistic phase density* $f(t,\mathbf{x},\mathbf{q}) \geq 0$ is the basic quantity of the kinetic theory. This function may be interpreted as giving the average number of particles with certain momentum at each time-space point. In the following we make use of the fact that the so called *volume element* d^3q/q_0 is invariant with respect to Lorentz-transformations.

Now we give the following definitions for the macroscopic moments and entropy four-vector and the definition of the macroscopic basic fields which we need for the formulation of the ultra-relativistic Euler equations, for more details see [16, 17].

(i) *Particle-density four-vector*:

$$N^\mu = N^\mu(t,\mathbf{x}) = \int_{\mathbb{R}^3} q^\mu\, f(t,\mathbf{x},\mathbf{q})\, \frac{d^3q}{q^0}. \tag{1.5}$$

(ii) *Energy-momentum tensor*:

$$T^{\mu\nu} = T^{\mu\nu}(t,\mathbf{x}) = m_0c^2 \int_{\mathbb{R}^3} q^\mu q^\nu\, f(t,\mathbf{x},\mathbf{q})\, \frac{d^3q}{q^0}, \tag{1.6}$$

with $\mu,\nu = 0,1,2,3$, ie these are total sixteen quanties.

(iii) *Entropy four-vector*:

$$S^\mu = S^\mu(t,\mathbf{x}) = -k_B \int_{\mathbb{R}^3} q^\mu\, f(t,\mathbf{x},\mathbf{q})\, \ln\left(\frac{f(t,\mathbf{x},\mathbf{q})}{\chi}\right) \frac{d^3q}{q^0}. \tag{1.7}$$

Here $k_B = 1.38062\times10^{-23} J/K$ is Boltzmann's constant and $\chi = (\frac{m_0c}{\hbar})^3$ with Planck's constant $\hbar = 1.05459\times10^{-34} Jsec$. Note that χ has the same dimension as f, namely 1/volume.

Tensor algebraic combinations of these moments:

(i) *The particle density*

$$n = \sqrt{N^\mu N_\mu}\,, \tag{1.8}$$

(ii) *the dimensionless velocity four-vector*

$$u^\mu = \frac{1}{n}\, N^\mu\,, \tag{1.9}$$

(iii) *the pressure and temperature*

$$p = \frac{1}{3}\,(u_\mu u_\nu - g_{\mu\nu})\, T^{\mu\nu} = k_B\, nT\,, \tag{1.10}$$

Remark:

The *macroscopic velocity* $\mathbf{v}$ of the gas can be obtained easily from the spatial part $\mathbf{u} = (u^1, u^2, u^3)^T$ of the dimensionless velocity four vector by

$$\mathbf{v} = c\,\frac{\mathbf{u}}{\sqrt{1+\mathbf{u}^2}}\,. \tag{1.11}$$

From this formula we can immediately read off that $|\mathbf{v}| < c$, i.e. the absolute value of the velocity is bounded by the speed of light. Note also that $u^0 = \sqrt{1+\mathbf{u}^2}$ is the Lorentz factor $\frac{1}{\sqrt{1-\mathbf{v}^2/c^2}}$. These definitions are valid for any relativistic phase-density $f = f(t, \mathbf{x}, \mathbf{q})$.

The most interesting aspect of the kinetic schemes is that instead of dealing with a system of nonlinear hyperbolic partial differential equations (for example relativistic Euler equations), we consider the collisionless transport equation of the kinetic theory of gases for developing upwind schemes. This relativistic linear transport equation without collision term

$$\frac{1}{c}\,\frac{\partial f}{\partial t} + \sum_{k=1}^{3} \frac{q^k}{q^0}\,\frac{\partial f}{\partial x^k} = 0 \tag{1.12}$$

is a linear transport equation for the scalar f. This equation gives the follwing conservation laws for the particle number, momentum and energy in differential form

$$\frac{\partial N^\mu}{\partial x^\mu} = 0\,, \qquad \frac{\partial T^{\mu\nu}}{\partial x^\mu} = 0 \quad \mu, \nu = 0, 1, 2, 3. \tag{1.13}$$

Further, when the basic unknown f in (1.12), the distribution function, is replaced by the relativistic Jüttner distribution function, see [16, 17], then the collisionless transport equation (1.12) is in general no longer valid, whereas the conservation laws (1.13) are still

satisfied and will reduce to the relativistic Euler equations. Apart from this if we take into account shock discontinuity then we need the weak form of conservation laws and entropy inequality as given below,

$$\oint_{\partial\Omega} N^{\nu}(t,\mathbf{x})do_{\nu} = 0,\ \oint_{\partial\Omega} T^{\mu\nu}(t,\mathbf{x})do_{\nu} = 0,\ \oint_{\partial\Omega} S^{\nu}(t,\mathbf{x})do_{\nu} \geq 0\,, \tag{1.14}$$

Here the covariant vector do_{ν} is a positively oriented surface element on the boundary $\partial\Omega$. It can be written in covariant form as

$$do_{\kappa} = \varepsilon_{\kappa\lambda\mu\nu} \sum_{i,j,m=1}^{3} \frac{\partial x^{\lambda}}{\partial u^{i}} \frac{\partial x^{\mu}}{\partial u^{j}} \frac{\partial x^{\nu}}{\partial u^{m}}\, du^{i}\, du^{j}\, du^{m}\,,$$

where $x^{\alpha} = x^{\alpha}(u^1, u^2, u^3)$ is a positively oriented parameterization of the boundary $\partial\Omega$.

In the following we will only consider dimensionless physical quantities corresponding to $k_B = 1\,,\ \hbar = 1$ and $c = 1$.

2 The Ultra-Relativistic Euler Equations

The three dimensional ultra-relativistic Euler equations derived in [16], can be written as

$$\frac{\partial W}{\partial t} + \sum_{k=1}^{3} \frac{\partial F^{k}(W)}{\partial x^{k}} = 0\,, \tag{2.1}$$

where

$$\begin{aligned} W &= \begin{pmatrix} N^{0} \\ T^{0i} \\ T^{00} \end{pmatrix} = \begin{pmatrix} n\sqrt{1+\mathbf{u}^2} \\ 4pu^{i}\sqrt{1+\mathbf{u}^2} \\ 3p + 4p\mathbf{u}^2 \end{pmatrix}, \\ F^{k}(W) &= \begin{pmatrix} N^{k} \\ T^{ik} \\ T^{0k} \end{pmatrix} = \begin{pmatrix} n\,u^{k} \\ p\,\delta^{ik} + 4pu^{i}u^{k} \\ 4pu^{k}\sqrt{1+\mathbf{u}^2} \end{pmatrix}. \end{aligned} \tag{2.2}$$

where $i = 1, 2, 3$ and the pressure $p = nT$.

In order to get the primitive variables n, u^k and p from the conserved variables W we use

$$
\begin{aligned}
p(t_n^+,\mathbf{x}) &= \frac{1}{3}\left[-T^{00}+\sqrt{4(T^{00})^2-3\sum_{k=1}^{3}(T^{0k})^2}\,\right],\\
u^k(t_n^+,\mathbf{x}) &= \frac{T^{0k}}{\sqrt{4p(t_n^+,\mathbf{x})[p(t_n^+,\mathbf{x})+T^{00}]}}, \quad k=1,2,3,\\
n(t_n^+,\mathbf{x}) &= \frac{N^0}{\sqrt{1+\sum_{k=1}^{3}[u^k(t_n^+,\mathbf{x})]^2}}.
\end{aligned}
\tag{2.3}
$$

Let us consider an initial distribution function $f_0(\mathbf{x},\mathbf{q}) \geq 0$. We wish to build a time approximation of (2.1) in the following way. We are given the initial data $n(0,\mathbf{x})$, $\mathbf{u}(0,\mathbf{x})$, $T(0,\mathbf{x})$ and we define the "equilibrium function" associated to these data by using the dimensionless relativistic Jüttner distribution function in the ultra-relativistic limit [16], which is given as

$$
\begin{aligned}
f_J(n,T,\mathbf{u},\mathbf{q}) &= \frac{n}{8\pi T^3}\,\exp\left(-\frac{u_\mu q^\mu}{T}\right)\\
&= \frac{n}{8\pi T^3}\,\exp\left(-\frac{|\mathbf{q}|}{T}\left(\sqrt{1+\mathbf{u}^2}-\mathbf{u}\cdot\frac{\mathbf{q}}{|\mathbf{q}|}\right)\right).
\end{aligned}
\tag{2.4}
$$

Using this distribution function we have

$$
nu^\mu = N^\mu(0,\mathbf{x}) = \int_{\mathbb{R}^3} q^\mu\, f_J(\mathbf{x},\mathbf{q})\,\frac{d^3q}{|\mathbf{q}|}\,,
\tag{2.5}
$$

$$
-p\,g^{\mu\nu} \,+\, 4pu^\mu u^\nu = T^{\mu\nu}(0,\mathbf{x}) = \int_{\mathbb{R}^3} q^\mu q^\nu\, f_J(\mathbf{x},\mathbf{q})\,\frac{d^3q}{|\mathbf{q}|}\,,
\tag{2.6}
$$

and the macroscopic *entropy four-vector*

$$
-N^\mu\,\ln\frac{n^4}{p^3}+\gamma N^\mu = S^\mu(0,\mathbf{x}) = -\int_{\mathbb{R}^3} q^\mu\, f_J(\mathbf{x},\mathbf{q})\,\ln f_J(\mathbf{x},\mathbf{q})\,\frac{d^3q}{|\mathbf{q}|}\,.
\tag{2.7}
$$

Then we solve the linear transport equation

$$
\begin{aligned}
&\frac{\partial f}{\partial t}+\sum_{k=1}^{3}\frac{q^k}{|\mathbf{q}|}\frac{\partial f}{\partial x^k}=0\,,\\
&f(0,\mathbf{x},\mathbf{q}) = f_0(\mathbf{x},\mathbf{q})\,.
\end{aligned}
\tag{2.8}
$$

The connection between the Boltzmann function f and macroscopic flow variables is

$$
\begin{aligned}
N^\mu(t,\mathbf{x}) &= \int_{\mathbb{R}^3} q^\mu\, f(t,\mathbf{x},\mathbf{q})\,\frac{d^3q}{|\mathbf{q}|}\,,\\
T^{\mu\nu}(t,\mathbf{x}) &= \int_{\mathbb{R}^3} q^\mu q^\nu\, f(t,\mathbf{x},\mathbf{q})\,\frac{d^3q}{|\mathbf{q}|}\,,
\end{aligned}
\tag{2.9}
$$

with macroscopic *entropy four-vector*

$$S^{\mu}(t,\mathbf{x}) = -\int_{\mathbb{R}^3} q^{\mu}\, f(t,\mathbf{x},\mathbf{q})\, \ln\left(\frac{f(t,\mathbf{x},\mathbf{q})}{\chi}\right) \frac{d^3q}{|\mathbf{q}|}\,. \tag{2.10}$$

which is first order (in Δt) approximaion of the solution to (2.1) for $t \leq \Delta t$.

The exact solution of the linear transport equation (2.8) is given by

$$f(t,\mathbf{x},\mathbf{q}) = f_0(x - t\frac{\mathbf{q}}{|\mathbf{q}|},\mathbf{q})\,. \tag{2.11}$$

Using (2.11) in (2.9) and (2.10) we get

$$\begin{aligned} N^{\mu}(t,\mathbf{x}) &= \int_{\mathbb{R}^3} q^{\mu}\, f_0(\mathbf{x} - t\frac{\mathbf{q}}{|\mathbf{q}|},\mathbf{q})\frac{d^3q}{|\mathbf{q}|}\,, \\ T^{\mu\nu}(t,\mathbf{x}) &= \int_{\mathbb{R}^3} q^{\mu}q^{\nu}\, f_0(\mathbf{x} - t\frac{\mathbf{q}}{|\mathbf{q}|},\mathbf{q})\frac{d^3q}{|\mathbf{q}|}\,, \end{aligned} \tag{2.12}$$

$$S^{\mu}(t,\mathbf{x}) = -\int_{\mathbb{R}^3} q^{\mu}\, (f_0 \ln f_0)(\mathbf{x} - t\frac{\mathbf{q}}{|\mathbf{q}|},\mathbf{q})\frac{d^3q}{|\mathbf{q}|}\,, \tag{2.13}$$

where f_0 is ultra-relativistic initial phase density at time $t = 0$

$$f_0(\mathbf{y},\mathbf{q}) = f_J(n(0,\mathbf{y}), T(0,\mathbf{y}), \mathbf{u}(0,\mathbf{y}), \mathbf{q})\,. \tag{2.14}$$

Now we can simplify the volume integrals (2.12) and (2.13) for the free flight moments. We can see in (2.14) that the fields $n(t,\mathbf{y})$, $T(t,\mathbf{y})$ and $\mathbf{u}(t,\mathbf{y})$ are not depending on $|\mathbf{q}|$ but only on the unit vector $\mathbf{w} = (w^1, w^2, w^3)^T = \frac{\mathbf{q}}{|\mathbf{q}|}$. This fact enables us to reduce the three-fold volume integrals to the two-fold surface integrals by applying polar coordinates, see [16] for more details. Furthermore if we introduce instead of the unit vector $\mathbf{w}$ the new variables $-1 \leq \xi \leq 1$ and $-\pi \leqq \varphi \leqq \pi$ by

$$w^1 = \xi\,, \qquad w^2 = \sqrt{1-\xi^2}\sin\varphi\,, \qquad w^3 = \sqrt{1-\xi^2}\cos\varphi\,, \tag{2.15}$$

then the simplified free-flight moments integrals for the one- and two-dimensional cases are given below, for more explanation see [16].

One dimensional moment integrals

Here we only consider solutions which depend on t and $x = x^1$ and satisfy $n = n(t,x)$, $\mathbf{u} = (u(t,x), 0, 0)$, $p = p(t,x)$. In this case the quantities n, T, u in the free flight phase density

are not depending on the variable φ. This fact enables us to carry out the integration with respect to φ directly. Thus the two-fold surface integrals reduces to simple $\xi-$integrals. For abbreviation we introduce

$$\Phi(y,\xi)=\frac{1}{2}\frac{n(y)}{(\sqrt{1+u^2(y)}-\xi u(y))^3}\,,\quad \Psi(y,\xi)=\frac{3}{2}\frac{(nT)(y)}{(\sqrt{1+u^2(y)}-\xi u(y))^4}\,. \tag{2.16}$$

Here we have supressed for simplicity the fixed time-argument t in the fields, which will not lead to confusions. The reduced integrals for the moments can be written as

$$W(t,x)=\begin{pmatrix} N^0(t,x)\\ T^{01}(t,x)\\ T^{00}(t,x)\end{pmatrix}=\int\limits_{-1}^{1}\begin{pmatrix}\Phi(x-t\xi,\xi)\\ \xi\,\Psi(x-t\xi,\xi)\\ \Psi(x-t\xi,\xi)\end{pmatrix}d\xi, \tag{2.17}$$

$$F^f(t,x)=\begin{pmatrix} N^1(t,x)\\ T^{11}(t,x)\\ T^{01}(t,x)\end{pmatrix}=\int\limits_{-1}^{1}\begin{pmatrix}\xi\,\Phi(x-t\xi,\xi)\\ \xi^2\,\Psi(x-t\xi,\xi)\\ \xi\,\Psi(x-t\xi,\xi)\end{pmatrix}d\xi\,. \tag{2.18}$$

$$\begin{aligned} S^0(t,x)&=-\int\limits_{-1}^{1}\eta(x-\tau\xi)\,\Phi(x-\tau\xi,\xi)\,d\xi\,,\\ S^1(t,x)&=-\int\limits_{-1}^{1}\xi\eta(x-\tau\xi)\,\Phi(x-\tau\xi,\xi)\,d\xi\,. \end{aligned} \tag{2.19}$$

where

$$\eta(y)=n(y)\left(\ln\left(\frac{n(y)}{8\pi T^3(y)}\right)-3\right)\,.$$

Two Dimensional moment integrals

In this case we consider the solutions which depend on $t,\ x=x^1$ and $y=x^2$ and satisfy $n=n(t,x,y)$, $\mathbf{u}=(u_1(t,x,y),u_2(t,x,y),0)$, $p=p(t,x,y)$. Instead of the unit vector $\mathbf{w}$, we use again the new variables in (2.15). For abbreviation we introduce with $\mathbf{y}\in\mathbb{R}^2$, where we have again supressed for simplicity the fixed time-argument t

$$\begin{aligned}\Phi(\mathbf{y},w^1,w^2)&=\frac{1}{4\pi}\frac{n(\mathbf{y})}{(\sqrt{1+(u_1^2+u_2^2)(\mathbf{y})}-u_1(\mathbf{y})\,w^1-u_2(\mathbf{y})\,w^2)^3}\,,\\ \Psi(\mathbf{y},w^1,w^2)&=\frac{3}{4\pi}\frac{(nT)(\mathbf{y})}{(\sqrt{1+(u_1^2+u_2^2)(\mathbf{y})}-u_1(\mathbf{y})\,w^1-u_2(\mathbf{y})\,w^2)^4}\,.\end{aligned}$$

Then the moment integrals take again a simplier form, namely

$$W(t,x,y) = \begin{pmatrix} N^0(t,x,y) \\ T^{01}(t,x,y) \\ T^{02}(t,x,y) \\ T^{00}(t,x,y) \end{pmatrix} = \int_{-\pi}^{\pi}\int_{-1}^{1} \begin{pmatrix} \Phi(x-tw^1, y-tw^2, w^1, w^2) \\ w^1\,\Psi(x-tw^1, y-tw^2, w^1, w^2) \\ w^2\,\Psi(x-tw^1, y-tw^2, w^1, w^2) \\ \Psi(x-tw^1, y-tw^2, w^1, w^2) \end{pmatrix} d\xi d\varphi\,, \quad (2.20)$$

$$F^f(t,x,y) = \begin{pmatrix} N^1(t,x,y) \\ T^{11}(t,x,y) \\ T^{12}(t,x,y) \\ T^{01}(t,x,y) \end{pmatrix} = \int_{-\pi}^{\pi}\int_{-1}^{1} \begin{pmatrix} w^1\,\Phi(x-tw^1, y-tw^2, w^1, w^2) \\ (w^1)^2\,\Psi(x-tw^1, y-tw^2, w^1, w^2) \\ w^1w^2\,\Psi(x-tw^1, y-tw^2, w^1, w^2) \\ w^1\,\Psi(x-tw^1, y-tw^2, w^1, w^2) \end{pmatrix} d\xi d\varphi\,, \quad (2.21)$$

$$G^f(t,x,y) = \begin{pmatrix} N^2(t,x,y) \\ T^{12}(t,x,y) \\ T^{22}(t,x,y) \\ T^{02}(t,x,y) \end{pmatrix} = \int_{-\pi}^{\pi}\int_{-1}^{1} \begin{pmatrix} w^2\,\Phi(x-tw^1, y-tw^2, w^1, w^2) \\ w^1w^2\,\Psi(x-tw^1, y-tw^2, w^1, w^2) \\ (w^2)^2\,\Psi(x-tw^1, y-tw^2, w^1, w^2) \\ w^2\,\Psi(x-tw^1, y-tw^2, w^1, w^2) \end{pmatrix} d\xi d\varphi\,.$$

The above one- and two-dimensional free-flight moments integrals will be used in order to derive a flux splitting scheme for the one- and two-dimensional ultra-relativistic Euler equations.

3 One-dimensional BGK-type KFVS Scheme

Here we want to solve the one dimensional Euler equations

$$\frac{\partial W}{\partial t} + \frac{\partial F(W)}{\partial x} = 0\,, \quad (3.1)$$

where

$$W = \begin{pmatrix} N^0 \\ T^{01} \\ T^{00} \end{pmatrix} = \begin{pmatrix} n\sqrt{1+u^2} \\ 4pu\sqrt{1+u^2} \\ 3p+4pu^2 \end{pmatrix}, \quad F(W) = \begin{pmatrix} N^1 \\ T^{11} \\ T^{01} \end{pmatrix} = \begin{pmatrix} n\,u \\ p+4pu^2 \\ 4pu\sqrt{1+u^2} \end{pmatrix}. \quad (3.2)$$

We start with a piecewise constant initial data $\overline{W}_i(0)$ over the cells $[x_{i-\frac{1}{2}}, x_{i+\frac{1}{2}}]$ of a given mesh size $\Delta x = x_{i+\frac{1}{2}} - x_{i-\frac{1}{2}}$, and we have to compute $\overline{W}_i(\Delta t)$ over the same cells. We take the natural CFL condition $\Delta t = \frac{\Delta x}{2}$ in order to ensure that neighbouring light-cones will not interact, see Figure 2. Note that in the theory of the classical Euler-equations one has to assume a bound for the characteristic speeds which depend on the choice of the initial data in order to obtain a CFL-condition. This is not necessary in our case, since every signal speed is bounded by the velocity of light.

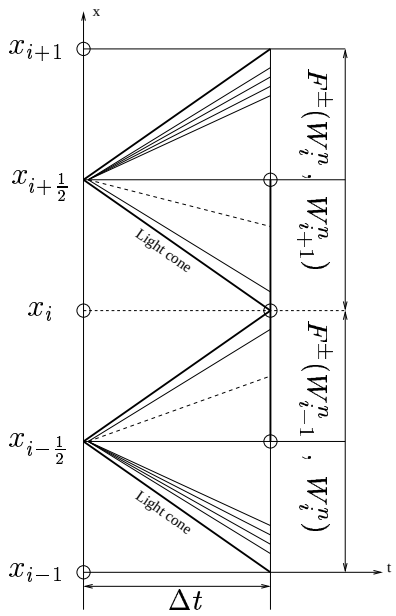

Figure 2: Illustration of the conservative kinetic scheme .

Using Figure 2, the one dimensional weak form of conservation laws $(1.14)_{1,2}$ over the domain $[0, \Delta t] \times [x_{i-\frac{1}{2}}, x_{i+\frac{1}{2}}]$ gives

$$\oint_{\partial\Omega} W(t,x)\,dx - F(W(t,x))\,dt = 0 \implies$$

$$\int_{x_{i-\frac{1}{2}}}^{x_{i+\frac{1}{2}}} [W(\Delta t, x) - W(0,x)]\,dx + \int_0^{\Delta t} \Big[F(\tau, x_{i+\frac{1}{2}}) - F(\tau, x_{i-\frac{1}{2}})\Big]\,d\tau = 0\,.$$

Let us define the integral mean values by

$$\overline{W}_i(t) = \frac{1}{\Delta x} \int_{x_{i-\frac{1}{2}}}^{x_{i+\frac{1}{2}}} W(t,x)dx\,.$$

Dividing the above balance equations by Δx, we get the following conservative formula

$$\overline{W}_i(\Delta t) = \overline{W}_i(0) - \frac{1}{\Delta x} \int_0^{\Delta t} \Big[F(\tau, x_{i+\frac{1}{2}}) - F(\tau, x_{i-\frac{1}{2}})\Big]\,d\tau\,, \tag{3.3}$$

with

$$F(\tau, x_{i+\frac{1}{2}}) = \eta F^f(\tau, x_{i+\frac{1}{2}}) + (1-\eta) F^e(\tau, x_{i+\frac{1}{2}})\,.$$

Here $F^f(\tau, x_{i+\frac{1}{2}})$ is given by (2.18) while we have to derive $F^e(\tau, x_{i+\frac{1}{2}})$. Also we will analyze the parameter η when we complete the derivation of the scheme for the 1D case.

From (2.18) we have

$$\int_0^{\Delta t} F^f(\tau, x_{i+\frac{1}{2}})\, d\tau = \int_0^{\Delta t}\int_{-1}^{1} f(x_{i+\frac{1}{2}} - \tau\xi, \xi)\, d\xi\, d\tau\,, \tag{3.4}$$

where

$$f(y,\xi) = \begin{pmatrix} \frac{1}{2}\frac{\xi\, n(y)}{(\sqrt{1+u^2(y)}-\xi u(y))^3} \\ \frac{3}{2}\frac{\xi^2\,(nT)(y)}{(\sqrt{1+u^2(y)}-\xi u(y))^4} \\ \frac{3}{2}\frac{\xi\,(nT)(y)}{(\sqrt{1+u^2(y)}-\xi u(y))^4} \end{pmatrix}.$$

The CFL condition states that ξ-integration is limited to ξ such that $|\xi|\tau \le \Delta x$. This means that $x_{i\pm\frac{1}{2}} - \xi\tau$ remains in a neighbour cell to $x_{i\pm\frac{1}{2}}$, see Figure 2. This implies that the field variables n, u, T in the splitted flux integrals will not depend on the $\xi-$integration, therefore equation (3.4) gives

$$\begin{aligned} F^f_{i+\frac{1}{2}} &= \frac{1}{\Delta t}\int_0^{\Delta t} F^f(\tau, x_{i+\frac{1}{2}})\, d\tau = \int_0^1 f(x_i,\xi)\, d\xi + \int_{-1}^0 f(x_{i+1},\xi)\, d\xi \\ &= F^+_i + F^-_{i+1}\,. \end{aligned} \tag{3.5}$$

where for each cell I_i

$$F^\pm_i = \begin{pmatrix} \pm\frac{n(x_i)}{4\sqrt{1+u^2(x_i)}}\left(\pm u(x_i) + \sqrt{1+u^2(x_i)}\right)^2 \\ \frac{p(x_i)}{2\sqrt{1+u^2(x_i)}}\left(\pm u(x_i) + \sqrt{1+u^2(x_i)}\right)^3 \\ \frac{p(x_i)}{4}\frac{\left(-u(x_i)\pm 3\sqrt{1+u^2(x_i)}\right)\left(\pm u(x_i)+\sqrt{1+u^2(x_i)}\right)^3}{1+u^2(x_i)} \end{pmatrix}, \tag{3.6}$$

where $p = nT$. This is exactly the kinetic flux vector splitting scheme for the ultra-relativistic Euler equations.

Now we are going to derive the equilibrium part of the flux $F^e_{i+\frac{1}{2}}$. As discussed in the introduction all FVS schemes based on positive (negative) particle velocities suffer from the same weakness. The particle free transport across cell interfaces unavoidably introduces a large numerical dissipation, and the viscosity and heat conduction coefficients are

proportional to the CFL time step. In order to reduce the over-diffusivity in flux splitting schemes, particles collisions have to be added in the transport process. Following the idea of Xu [37], the aim is to obtain an equilibrium state $\overline{W}^e_{i+\frac{1}{2}}$ at the cell interface by combining the left and right moving beams. Using this equilibrium state, we get an equilibrium flux funtion $F^e_{i+\frac{1}{2}}$ through the flux function definition $(3.2)_2$.

As a simple particle collisional model, we can imagine that the particles from the left- and right-hand sides of a cell interface collapse totally to form an equilibrium state. In order to define the equilibrium state at the cell interface, we need first to figure out the corresponding macroscopic quantities $\overline{W}^e_{i+\frac{1}{2}}$ there, which are the combination of the total mass, momentum and energy of the left and right moving beams. Now using (2.17) we have

$$\overline{W}^e_{i+\frac{1}{2}} = \begin{pmatrix} \overline{N}^0 \\ \overline{T}^{01} \\ \overline{T}^{00} \end{pmatrix}_{i+\frac{1}{2}} = \begin{pmatrix} N^0 \\ T^{01} \\ T^{00} \end{pmatrix}^+_i + \begin{pmatrix} N^0 \\ T^{01} \\ T^{00} \end{pmatrix}^-_{i+1}, \tag{3.7}$$

where for each cell I_i

$$\begin{pmatrix} N^0 \\ T^{01} \\ T^{00} \end{pmatrix}^\pm_i = \begin{pmatrix} \frac{n(x_i)\left(2\sqrt{1+u^2(x_i)} \mp u(x_i)\right)}{4(1+u^2(x_i))\left(u(x_i) \mp \sqrt{1+u^2(x_i)}\right)^2} \\ \frac{p(x_i)}{4} \frac{\left(-u(x_i) \pm 3\sqrt{1+u^2(x_i)}\right)\left(\pm u(x_i) + \sqrt{1+u^2(x_i)}\right)^3}{1+u^2(x_i)} \\ \frac{p(x_i)\left(3+4u^2(x_i) \mp 3u(x_i)\sqrt{1+u^2(x_i)}\right)}{2\left(1+u^2(x_i) \mp u(x_i)\sqrt{1+u^2(x_i)}\right)^3} \end{pmatrix}. \tag{3.8}$$

Now we use the following relation in order to get the averaged values of the primitive variables from the above averaged conservative variables in (3.7),

$$p = \frac{1}{3}\left[-\overline{T}^{00} + \sqrt{4(\overline{T}^{00})^2 - 3(\overline{T}^{01})^2}\right], \quad u = \frac{\overline{T}^{01}}{\sqrt{4p[p+\overline{T}^{00}]}}, \quad n = \frac{\overline{N}^0}{\sqrt{1+u^2}}. \tag{3.9}$$

Then from these "averaged" macroscopic flow quantities in the equation (3.9), we can construct the equilibrium flux function

$$F^e_{i+\frac{1}{2}} = \frac{1}{\Delta t}\int_0^{\Delta t} F^e(\tau, x_{i+\frac{1}{2}})\, d\tau = \begin{pmatrix} n\,u \\ p + 4pu^2 \\ 4pu\sqrt{1+u^2} \end{pmatrix}_{i+\frac{1}{2}}. \tag{3.10}$$

Using (3.5) and (3.10) in (3.3) we finally get the following upwind kinetic scheme

$$\overline{W}_i(\Delta t) = \overline{W}_i(0) - \frac{\Delta t}{\Delta x}\left[F_{i+\frac{1}{2}} - F_{i-\frac{1}{2}}\right], \tag{3.11}$$

with

$$F_{i+\frac{1}{2}} = \eta F^f_{i+\frac{1}{2}} + (1-\eta) F^e_{i+\frac{1}{2}}\,, \tag{3.12}$$

where η is an adaptive parameter. For a first order scheme η can be fixed, such as 0.7 or 0.5, in the numerical calculations. Theoretically, the parameter η should depend on the real flow situations: in the equilibrium and smooth flow regions, the use of $\eta \sim 0$ is physically reasonable, and in discontinuity region, η should be close to 1 in order to have enough numerical dissipation to recover the smooth shock transition. A possible choice for η in high order scheme is to consider it as a function of the pressure difference, such as the switch function in the JST scheme [7]. We follow the MUSCL-type approach to extend the current scheme to high order. For the high-order scheme, the interpolated pressure jump p_l and p_r around a cell interface can naturally be used as a switch function for the parameter η, such as

$$\eta = 1 - \mathrm{Exp}\left(-\frac{|p_l - p_r|}{p_l + p_r}\right)\,,$$

where α can be some constant, see Xu [38]. In order to get back the premitive vsriables n, u, T in (3.11) we use again (3.9).

3.1 Second Order Extension of the Scheme in 1D

In order to get the second order accuracy we have the following three steps.

(I): **Data Reconstruction.** Starting with a piecewise-constant solution in time and space, $\sum \overline{W}_i(0)\chi_i(x)$, one reconstruct a piecewise linear (MUSCL-type) approximation in space, namely

$$W(0,x) = \sum \left[\overline{W}_i(0) + W_i^x \frac{(x-x_i)}{\Delta x}\right] \chi_i(x)\,. \tag{3.13}$$

Here, $\chi_i(x)$ is the characteristic function of the cell, $I_i := \{\xi \mid |\xi - x_i| \le \frac{\Delta x}{2}\}$, centered arround $x_i = i\Delta x$, and W_i^x abbreviates a first-order discrete slopes.

The extreme points $x = 0$ and $x = \Delta x$, in local coordinates correspond to the intercell boundaries in general coordinates $x_{i-\frac{1}{2}}$ and $x_{i+\frac{1}{2}}$, respectively, see Figure 3. The values W_i at the extreme points are

$$W_i^L = \overline{W}_i(0) - \frac{1}{2}W_i^x\,, \quad W_i^R = \overline{W}_i(0) + \frac{1}{2}W_i^x \tag{3.14}$$

and are usually called *boundary extrapolated values.*

A possible computation of these slopes, which results in an overall nonoscillatory schemes (consult [31]), is given by family of *discrete derivatives* parameterized with $1 \leq \theta \leq 2$, i.e., for any grid function $\{W_i\}$ we set

$$W_i^x = MM\theta\{W_{i-1}, W_i, W_{i+1}\} = MM\left(\theta\Delta W_{i+\frac{1}{2}}, \frac{\theta}{2}(\Delta W_{i-\frac{1}{2}} + \Delta W_{i+\frac{1}{2}}), \theta\Delta W_{i-\frac{1}{2}}\right) .$$

Here, Δ denotes the central differencing, $\Delta W_{i+\frac{1}{2}} = W_{i+1} - W_i$, and MM denotes the min-mod nonlinear limiter

$$MM\{x_1, x_2, ...\} = \begin{cases} \min_i\{x_i\} & \text{if } x_i > 0 \quad \forall i\,, \\ \max_i\{x_i\} & \text{if } x_i < 0 \quad \forall i\,, \\ 0 & \text{otherwise}\,. \end{cases} \tag{3.15}$$

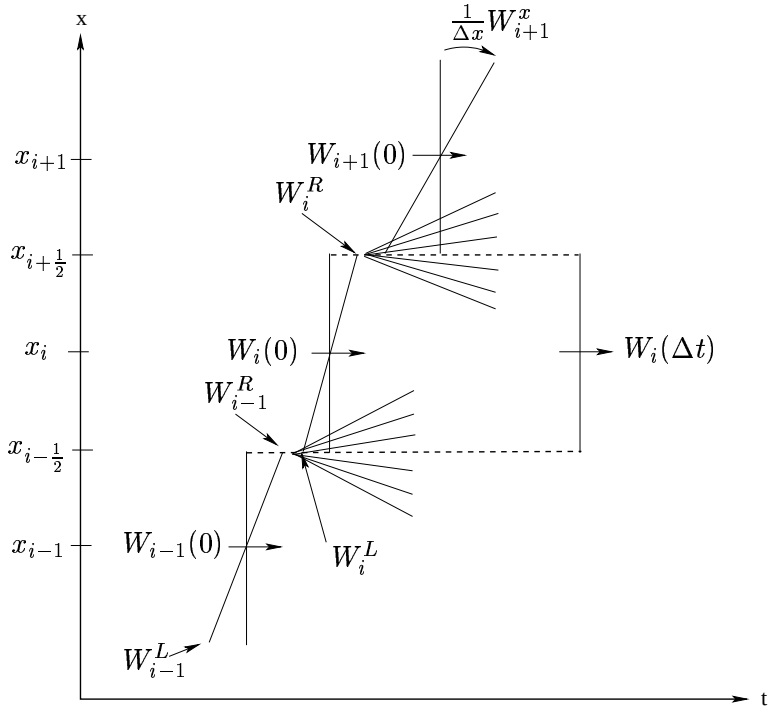

Figure 3: Second Order Reconstruction

This interpolant, (3.13), is then evolved exactly in time and projected on the cell-averages at the next time step.

(II): **Evolution.** For each cell I_i, the boundary extrapolated values W_i^L, W_i^R in (3.14) are evolved for a time $\frac{1}{2}\Delta t$ by

$$\hat{W}_i^L = W_i^L + \frac{1}{2}\frac{\Delta t}{\Delta x}\left[F(W_i^L) - F(W_i^R)\right] ,$$
$$\hat{W}_i^R = W_i^R + \frac{1}{2}\frac{\Delta t}{\Delta x}\left[F(W_i^L) - F(W_i^R)\right] , \tag{3.16}$$

where F is the force term from in the Euler equations $(3.2)_2$.

Note that this evolution step is entirely contained in each cell I_i, as the intercell fluxes are evaluated at the boundary extrapolated values of each cell. At each intercell position $i + \frac{1}{2}$ there are two fluxes, namely W_i^R and W_{i+1}^L, which are in general distinct. This does not really affect the *conservative* character of the overall method, as this step is only an intermediate step [31].

(III): Finally we use the conservative formula (3.11) in order to get the conservative variables at next time step

$$\overline{W}_i(\Delta t) = \overline{W}_i(0) - \frac{\Delta t}{\Delta x}\left[F_{i+\frac{1}{2}} - F_{i-\frac{1}{2}}\right] , \tag{3.17}$$

with

$$F_{i+\frac{1}{2}} = \eta F^f_{i+\frac{1}{2}} + (1-\eta)F^e_{i+\frac{1}{2}} , \tag{3.18}$$

where $F^f_{i+\frac{1}{2}} = F^+(\hat{W}_i^R) + F^-(\hat{W}_{i+1}^L)$, and $F^\pm$ is given by (3.6).

Similarly to calculate $F^e_{i+\frac{1}{2}}$, we have

$$\overline{W}^e_{i+\frac{1}{2}} = (\hat{W}^+)_i^R + (\hat{W}^-)_{i+1}^L ,$$

using (3.16) $\hat{W}_i^\pm$ can be calculated from (3.8), then

$$F^e_{i+\frac{1}{2}} = F^e(\overline{W}^e_{i+\frac{1}{2}}) .$$

In order to get back the fields n, u_1, u_2, T we use the relations (3.9).

4 Two-Dimensional BGK-type KFVS Scheme

Here we want to solve the two-dimensional Euler equations

$$\frac{\partial W}{\partial t} + \frac{\partial F(W)}{\partial x} + \frac{\partial G(W)}{\partial y} = 0 , \tag{4.1}$$

where

$$W = \begin{pmatrix} N^0 \\ T^{01} \\ T^{02} \\ T^{00} \end{pmatrix} = \begin{pmatrix} n\sqrt{1+\mathbf{u}^2} \\ 4p\,u1\sqrt{1+\mathbf{u}^2} \\ 4p\,u2\sqrt{1+\mathbf{u}^2} \\ 3p+4p\,\mathbf{u}^2 \end{pmatrix}, \; F(W) = \begin{pmatrix} N^1 \\ T^{11} \\ T^{12} \\ T^{01} \end{pmatrix} = \begin{pmatrix} n\,u_1 \\ p+4p\,u_1^2 \\ 4p\,u_1\,u_2 \\ 4p\,u_1\sqrt{1+\mathbf{u}^2} \end{pmatrix},$$

$$G(W) = \begin{pmatrix} N^2 \\ T^{12} \\ T^{22} \\ T^{02} \end{pmatrix} = \begin{pmatrix} n\,u_2 \\ 4p\,u_1\,u_2 \\ p+4p\,u_2^2 \\ 4p\,u_2\sqrt{1+\mathbf{u}^2} \end{pmatrix}, \tag{4.2}$$

where $\mathbf{u} = \sqrt{1+u_1^2+u_2^2}$. We start again with a piecewise constant initial data of the conservative variables $\overline{W}_{i,j}(0)$. Using the weak conservation laws $(1.14)_{1,2}$ in two-dimensional case over the volume $[0,\Delta t]\times[x_{i-\frac{1}{2}},x_{i+\frac{1}{2}}]\times[y_{j-\frac{1}{2}},y_{j+\frac{1}{2}}]$, we get

$$\overline{W}_{i,j}(\Delta t) = \overline{W}_{i,j}(0) - \frac{\Delta t}{\Delta x}\left[F_{i+\frac{1}{2},j} - F_{i-\frac{1}{2},j}\right] - \frac{\Delta t}{\Delta y}\left[G_{i,j+\frac{1}{2}} - G_{i,j-\frac{1}{2}}\right], \tag{4.3}$$

where

$$\overline{W}_{i,j}(t) = \frac{1}{\Delta x\Delta y}\int\limits_{x_{i-\frac{1}{2}}}^{x_{i+\frac{1}{2}}}\int\limits_{y_{j-\frac{1}{2}}}^{y_{j+\frac{1}{2}}} W(t,x,y)\,dxdy\,,$$

$$F_{i+\frac{1}{2},j} = \eta F^f_{i+\frac{1}{2},j} + (1-\eta)F^e_{i+\frac{1}{2},j}\,, \;\; G_{i,j+\frac{1}{2}} = \eta G^f_{i,j+\frac{1}{2}} + (1-\eta)G^e_{i,j+\frac{1}{2}}\,.$$

Here

$$F^f_{i+\frac{1}{2},j} = \frac{1}{\Delta t}\int\limits_0^{\Delta t} F^f(\tau, x_{i+\frac{1}{2}}, y_j)\,d\tau\,, \quad G^f_{i,j+\frac{1}{2}} = \frac{1}{\Delta t}\int\limits_0^{\Delta t} G^f(\tau, x_i, y_{j+\frac{1}{2}})\,d\tau\,,$$

where the flux moments $F^f(\tau, x_{i+\frac{1}{2}}, y_j)$ and $G^f(\tau, x_i, y_{j+\frac{1}{2}})$ are given in (2.21).

If the CFL condition $\Delta t \le \frac{1}{2}min(\Delta x,\Delta y)$ is satisfied, then we can utilize the kinetic flux vector splitting (KFVS). Since after flux splitting the fields n, u_1, u_2 and T in (2.20) and (2.21) are not depending on the integration variables ξ and φ, therefore we can solve analytically these moments integrals for the fluxes. This gives

$$F^f_{i+\frac{1}{2},j} = F^+_{i,j} + F^-_{i+1,j}\,, \qquad G^f_{i,j+\frac{1}{2}} = G^+_{i,j} + F^-_{i,j+1}\,. \tag{4.4}$$

where from (2.21)

$$F^\pm_{i,j} = \begin{pmatrix} N^1 \\ T^{11} \\ T^{12} \\ T^{01} \end{pmatrix}^\pm_{i,j}, \quad G^\pm = \begin{pmatrix} N^2 \\ T^{12} \\ T^{22} \\ T^{02} \end{pmatrix}^\pm_{i,j}.$$

Here for the fluxes $F^{\pm}_{i,j}$ we split the integrals with respect to variable ξ and take the integration with respect to variable φ as a whole. While for the fluxes $G^{\pm}_{i,j}$, we split the integrals with respect to variable φ and integrate the integrals with respect to ξ as a whole. Thus we get the following relations for the fluxes $F^{\pm}_{i,j}$ and $G^{\pm}_{i,j}$ for each cell $I_{i,j}$

$$F^{\pm}_{i,j} = \begin{pmatrix} \frac{nu_1}{2} \pm \frac{n(1+2u_1^2)}{4\sqrt{1+u_1^2}} \\ \frac{p(1+4u_1^2)}{2} \pm \frac{pu_1(3+4u_1^2)}{2\sqrt{1+u_1^2}} \\ 2pu_1u_2 \pm \frac{pu_2(3+12u_1^2+8u_1^4)}{4(1+u_1^2)^{\frac{3}{2}}} \\ p\sqrt{1+\mathbf{u}^2}\left(2u_1 \pm \frac{(3+12u_1^2+8u_1^4)}{4(1+u_1^2)^{\frac{3}{2}}}\right) \end{pmatrix}_{i,j},$$

$$G^{\pm}_{i,j} = \begin{pmatrix} \frac{nu_2}{2} \pm \frac{n(1+2u_2^2)}{4\sqrt{1+u_2^2}} \\ 2pu_1u_2 \pm \frac{pu_2(3+12u_1^2+8u_1^4)}{4(1+u_1^2)^{\frac{3}{2}}} \\ \frac{p(1+4u_2^2)}{2} \pm \frac{pu_2(3+4u_2^2)}{2\sqrt{1+u_2^2}} \\ p\sqrt{1+\mathbf{u}^2}\left(2u_2 \pm \frac{(3+12u_2^2+8u_2^4)}{4(1+u_2^2)^{\frac{3}{2}}}\right) \end{pmatrix}_{i,j}. \tag{4.5}$$

where $\mathbf{u} = \sqrt{u_1^2+u_2^2}$.

As discussed in the introduction and in one dimensional case, all FVS schemes based on positive (negative) particle velocities suffer from the same weakness. The particle free transport across the cell interfaces unavoidably introduces a large numerical dissipation, and the viscosity and heat conduction coefficients are proportional to the CFL time step. In order to reduce the over-diffusivity in flux splitting schemes, particle collisions have to be added in the transport process.

As a simple particle collisional model, we can imagine that the particles at the cell interface moving in positive and negative $x-$ and $y-$ directions collapse totally to form an equilibrium state. In order to define the equilibrium state at the cell interface, we need first to figure out the corresponding macroscopic quantities $\overline{W}^e_{i+\frac{1}{2},j}$ and $\overline{W}^e_{i,j+\frac{1}{2}}$ there, which are the combination of the total mass, momentum and energy of the moving beams in negative and positive direction of x- and y-axis. Now using (2.20) we have

$$\overline{W}^e_{i+\frac{1}{2},j} = \begin{pmatrix} \overline{N}^0 \\ \overline{T}^{01} \\ \overline{T}^{02} \\ \overline{T}^{00} \end{pmatrix}_{i+\frac{1}{2},j} = \begin{pmatrix} N^0 \\ T^{01} \\ T^{02} \\ T^{00} \end{pmatrix}^{+}_{i,j} + \begin{pmatrix} N^0 \\ T^{01} \\ T^{02} \\ T^{00} \end{pmatrix}^{-}_{i+1,j},$$

where for each cell $I_{i,j}$

$$\begin{pmatrix} N^0 \\ T^{01} \\ T^{02} \\ T^{00} \end{pmatrix}^{\pm}_{i,j} = \begin{pmatrix} \frac{n\sqrt{1+\mathbf{u}^2}}{2}\left(1 \pm \frac{u_1(3+2u_1^2)}{2(1+u_1^2)^{\frac{3}{2}}}\right) \\ p\sqrt{1+\mathbf{u}^2}\left(2u_1 \pm \frac{(3+12u_1^2+8u_1^4)}{4(1+u_1^2)^{\frac{3}{2}}}\right) \\ pu_2\sqrt{1+\mathbf{u}^2}\left(2 \pm \frac{u_1(15+20u_1^2+8u_1^4)}{4(1+u_1^2)^{\frac{5}{2}}}\right) \\ \frac{p\left(3+4\mathbf{u}^2\right)}{2} \pm \frac{pu_1\left(12+15(u_1^2+\mathbf{u}^2)+8u_1^4\mathbf{u}^2+2u_1^2(3u_1^2+10\mathbf{u}^2)\right)}{4(1+u_1^2)^{\frac{5}{2}}} \end{pmatrix}_{i,j} . \tag{4.6}$$

Similarly

$$\overline{W}^e_{i,j+\frac{1}{2}} = \begin{pmatrix} \overline{N}^0 \\ \overline{T}^{01} \\ \overline{T}^{02} \\ \overline{T}^{00} \end{pmatrix}_{i,j+\frac{1}{2}} = \begin{pmatrix} N^0 \\ T^{01} \\ T^{02} \\ T^{00} \end{pmatrix}^{+}_{i,j} + \begin{pmatrix} N^0 \\ T^{01} \\ T^{02} \\ T^{00} \end{pmatrix}^{-}_{i,j+1} ,$$

where for each cell $I_{i,j}$

$$\begin{pmatrix} N^0 \\ T^{01} \\ T^{02} \\ T^{00} \end{pmatrix}^{\pm}_{i,j} = \begin{pmatrix} \frac{n(x_i)\sqrt{1+\mathbf{u}^2}}{2}\left(1 \pm \frac{u_2(3+2u_2^2)}{2(1+u_2^2)^{\frac{3}{2}}}\right) \\ pu_1\sqrt{1+\mathbf{u}^2}\left(2 \pm \frac{u_2(15+20u_2^2+8u_2^4)}{4(1+u_2^2)^{\frac{5}{2}}}\right) \\ p\sqrt{1+\mathbf{u}^2}\left(2u_2 \pm \frac{(3+12u_2^2+8u_2^4)}{4(1+u_2^2)^{\frac{3}{2}}}\right) \\ \frac{p\left(3+4\mathbf{u}^2\right)}{2} \pm \frac{pu_2\left(12+15(u_2^2+\mathbf{u}^2)+8u_2^4\mathbf{u}^2+2u_2^2(3u_2^2+10\mathbf{u}^2)\right)}{4(1+u_2^2)^{\frac{5}{2}}} \end{pmatrix}_{i,j} . \tag{4.7}$$

where $\mathbf{u} = \sqrt{u_1^2+u_2^2}$.

Now we use the following relation in order to get the averaged values of the primitive variables from the above averaged conservative variables

$$\begin{aligned} p &= \frac{1}{3}\left[-\overline{T}^{00} + \sqrt{4(\overline{T}^{00})^2 - 3\left[(\overline{T}^{01})^2 + (\overline{T}^{02})^2\right]}\right] , \\ u_1 &= \frac{\overline{T}^{01}}{\sqrt{4p[p+\overline{T}^{00}]}} , \quad u_2 = \frac{\overline{T}^{02}}{\sqrt{4p[p+\overline{T}^{00}]}} , \quad n = \frac{\overline{N}^0}{\sqrt{1+u_1^2+u_2^2}} . \end{aligned} \tag{4.8}$$

Then from these "averaged" macroscopic flow quantities in the equation (4.8), we can construct the equilibrium flux functions

$$F^e_{i+\frac{1}{2},j} = \frac{1}{\Delta t}\int_0^{\Delta t} F^e(\tau, x_{i+\frac{1}{2}}, y_j)\, d\tau = \begin{pmatrix} n\,u_1 \\ p + 4p\,u_1^2 \\ 4p\,u_1\,u_2 \\ 4p\,u_1\sqrt{1+u_1^2+u_2^2} \end{pmatrix}_{i+\frac{1}{2},j}, \tag{4.9}$$

$$G^e_{i,j+\frac{1}{2}} = \frac{1}{\Delta t}\int_0^{\Delta t} F^e(\tau, x_i, y_{j+\frac{1}{2}})\, d\tau = \begin{pmatrix} n\,u_2 \\ 4p\,u_1\,u_2 \\ p + 4p\,u_2^2 \\ 4p\,u_2\sqrt{1+u_1^2+u_2^2} \end{pmatrix}_{i,j+\frac{1}{2}}. \tag{4.10}$$

Using (4.4), (4.9) and (4.10) in (4.3) we finally get the following upwind kinetic scheme

$$\overline{W}_{i,j}(\Delta t) = \overline{W}_{i,j}(0) - \frac{\Delta t}{\Delta x}\left[F_{i+\frac{1}{2},j} - F_{i-\frac{1}{2},j}\right] - \frac{\Delta t}{\Delta y}\left[G_{i,j+\frac{1}{2}} - G_{i,j-\frac{1}{2}}\right], \tag{4.11}$$

with

$$F_{i+\frac{1}{2},j} = \eta F^f_{i+\frac{1}{2},j} + (1-\eta)F^e_{i+\frac{1}{2},j}\,,\ G_{i,j+\frac{1}{2}} = \eta G^f_{i,j+\frac{1}{2}} + (1-\eta)G^e_{i,j+\frac{1}{2}}\,, \tag{4.12}$$

again η is an adaptive parameter and can be taken fixed, for example 0.5 or 0.7. It can also be calculated from the left and right state pressure at the cell interface by using the relation

$$\eta = 1 - \mathrm{Exp}\left(-\alpha\frac{|p_l - p_r|}{p_l + p_r}\right).$$

The value of η should be such that it allow a smooth transition of shocks, while resolve the contact discontinuities sufficiently. In order to get back the fields n, u_1, u_2, T from the conservative variable at next time we use the relations (4.8).

4.1 Second Order Extension of the Scheme in 2D

Here we present the second-order MUSCL-type approach for the two-dimensional case. Keeping in view the MUSCL approach discussed in the previous section for the one-dimensional case, we have again the following three steps.

(I): **Data Reconstruction and Boundary Extrapolated Values.** Starting with a piecewise-constant solution in time and space, $\overline{W}_{i,j}(0)$, one reconstruct a piecewise linear (MUSCL-type) approximation independently in x- and y-directions by selecting

selecting respective slope vectors (differences) W^x and W^y. Boundary extrapolated values are

$$W^{LX}_{i,j} = \overline{W}_{i,j}(0) - \frac{1}{2}W^x_{i,j}\,, \quad W^{RX}_{i,j} = \overline{W}_{i,j}(0) + \frac{1}{2}W^x_{i,j}\,,$$
$$W^{LY}_{i,j} = \overline{W}_{i,j}(0) - \frac{1}{2}W^y_{i,j}\,, \quad W^{RY}_{i,j} = \overline{W}_{i,j}(0) + \frac{1}{2}W^y_{i,j}\,. \tag{4.13}$$

A possible computation of these slopes, is given by family of *discrete derivatives* parameterized with $1 \le \theta \le 2$, for example

$$W^x_{i,j} = MM\left\{\theta\Delta\overline{W}_{i+\frac{1}{2},j}, \frac{\theta}{2}\left(\Delta\overline{W}_{i+\frac{1}{2},j} + \Delta\overline{W}_{i-\frac{1}{2},j}\right), \theta\Delta\overline{W}_{i-\frac{1}{2},j}\right\}\,,$$
$$W^y_{i,j} = MM\left\{\theta\Delta\overline{W}_{i,j+\frac{1}{2}}, \frac{\theta}{2}\left(\Delta\overline{W}_{i,j+\frac{1}{2}} + \Delta\overline{W}_{i,j-\frac{1}{2}}\right), \theta\Delta\overline{W}_{i,j-\frac{1}{2}}\right\}\,.$$

Here Δ denotes central differencing,

$$\Delta\overline{W}_{i+\frac{1}{2},j} = \overline{W}_{i+1,j} - \overline{W}_{i,j}, \qquad \Delta\overline{W}_{i,j+\frac{1}{2}} = \overline{W}_{i,j+1} - \overline{W}_{i,j}\,,$$

and MM denotes the min-mod nonlinear limiter

$$MM\{x_1, x_2, ...\} = \begin{cases} \min_i\{x_i\} & \text{if } x_i > 0 \quad \forall i\,, \\ \max_i\{x_i\} & \text{if } x_i < 0 \quad \forall i\,, \\ 0 & \text{otherwise}\,. \end{cases} \tag{4.14}$$

(II): **Evolution of Boundary Extrapolated Values.** The boundary extrapolated values are evolved at a time $\frac{\Delta t}{2}$ by using

$$\hat{W}^l_{i,j} = W^l_{i,j} + \frac{1}{2}\frac{\Delta t}{\Delta x}\left[F(W^{LX}_{i,j}) - F(W^{RX}_{i,j})\right] + \frac{1}{2}\frac{\Delta t}{\Delta y}\left[G(W^{LY}_{i,j}) - G(W^{RY}_{i,j})\right]\,, \tag{4.15}$$

for $l = LX, RX, LY, RY$. Here the values of F and G are obtained from the Euler equations $(4.2)_{2,3}$.

(III): **Solution at the Next Time Step.** At each intercell position one solves

$$\overline{W}_{i,j}(\Delta t) = \overline{W}_{i,j}(0) - \frac{\Delta t}{\Delta x}\left[F_{i+\frac{1}{2},j} - F_{i+\frac{1}{2},j}\right] - \frac{\Delta t}{\Delta y}\left[G_{i,j+\frac{1}{2}} - G_{i,j+\frac{1}{2}}\right]\,,$$

with

$$F_{i+\frac{1}{2},j} = \eta F^f_{i+\frac{1}{2},j} + (1-\eta)F^e_{i+\frac{1}{2},j}\,, \; G_{i,j+\frac{1}{2}} = \eta G^f_{i,j+\frac{1}{2}} + (1-\eta)G^e_{i,j+\frac{1}{2}}\,, \tag{4.16}$$

where

$$F^f_{i+\frac{1}{2},j} = F^+(\hat{w}^{RX}_{i,j}) + F^-(\hat{w}^{LX}_{i+1,j})\,, \; G^f_{i,j+\frac{1}{2}} = G^+(\hat{w}^{RY}_{i,j}) + G^-(\hat{w}^{LY}_{i,j+1})$$

where $F^{\pm}$ and $G^{\pm}$ are given by (4.5).

Similarly to calculate $F^e_{i+\frac{1}{2},j}$ and $G^e_{i,j+\frac{1}{2}}$, we have

$$\overline{W}^e_{i+\frac{1}{2},j} = (\hat{W}^+)^{RX}_{i,j} + (\hat{W}^-)^{LX}_{i+1,j}\,, \quad \overline{W}^e_{i,j+\frac{1}{2}} = (\hat{W}^+)^{RY}_{i,j} + (\hat{W}^-)^{LY}_{i,j+1}\,,$$

using (4.15) $\hat{W}^{\pm}$ can be obtained from (4.6) for $\overline{W}_{i+\frac{1}{2},j}$ and by (4.7) for $\overline{W}_{i,j+\frac{1}{2}}$, then we have

$$F^e_{i+\frac{1}{2},j} = F^e(\overline{W}^e_{i+\frac{1}{2},j})\,, \quad G^e_{i,j+\frac{1}{2}} = G^e(\overline{W}^e_{i,j+\frac{1}{2}})\,.$$

In order to get back the fields n, u_1, u_2, T we use the relations (4.8).

5 Conclusions

In this paper we have derived BGK-type KFVS scheme for the ultra-relativistic Euler equatons. The numerical flux function is constructed with consideration of particle transport across the cell interface and particle "collisions" are implemented in the transport process to reduce the numerical dissipation, especially at the contact discontinuity. The parameter η, which determines the weights between the free transport and equilibrium fluxes takes constant values in the current study.

It is well known that, oftenly the requirement for robustness and accuracy in the design of a numerical scheme are in conflict with each other. If a scheme is robust, it is unnecessarily diffusive and if a scheme is accurate, it loses robustness. In order to get a correct representation of flow motion in the discritized space and time, a consistent dissipative mechanism must be added in the gas evolution stage. An optimum choice in our case is to take a combination of both free-flights and collisions. In shock region we need more dissipation for smooth transition of shock while at the contact discontinuity we need more collisions (equilibrium case) to get a good resolution of the contact discontinuity. In this paper we have used a convex combination of the collisional and and collisionless fluxes with η as an adaptive parameter. The results from the test cases shows that this procedure worked well.

From the numerical case studies it was found that both KFVS and BGK-type KFVS schemes for the ultra-relativistic Euler equations give comparable results to the Godunov and central schemes. Also we found that BGK-type KFVS scheme for gives better resolution at the contact discontinuity as compared to the KFVS scheme.

Although we have restricted our attension to one- and two-dimensional cases in the current paper, the extension of the current method to three space dimensions is analogous.

6 Numerical Test Cases

Here we present some one- and two-dimensional numerical examples. We compare the results of BGK-type KFVS scheme with exact solution, Godunov scheme, KFVS scheme and central scheme. The results shows that both BGK-type and KFVS schemes give comparable results to the Godunov and central schemes.

Problem 1: In this test problem we consider the time evolution of an initial discontinuous state of a fluid moving in opposite directions. The intial data are

$$(n, u, p) = \begin{cases} (1.0, 1.0, 3.0) & \text{if } x < 0.5\,, \\ (1.0, -0.5, 2.0) & \text{if } x \geq 0.5\,. \end{cases}$$

This problem consist of a left shock, a contact and a right shock. The results at $t = 0.5$ are shown in Figures 4 and 5 for 400 mesh points.

Problem 2: In this test problem we consider the time evolution of an initial discontinuous state of a fluid at rest. The intial data are

$$(n, u, p) = \begin{cases} (5.0, 0.0, 10.0) & \text{if } x < 0.5\,, \\ (1.0, 0.0, 0.5) & \text{if } x \geq 0.5\,. \end{cases}$$

This problem involves the formation of an intermediate state bounded by a shock wave propagating to the right and a transonic rarefaction wave propagating to the left. The fluid in the intermediate state moves at a mildly relativistic speed ($v = 0.58c$) to the right. Flow particles accumulate in a dense shell behind the shock wave compressing the fluid and heating it. The fluid is extremely relativistic from thermodynamic point of view, but only mildly relativistic dynamically. Figures 6 and 7 shows the results at $t = 0.5$ for 400 mesh points.

Problem 3: The intial dare are

$$(n, u, p) = \begin{cases} (1.0, -0.5, 2.0) & \text{if } x < 0.5\,, \\ (1.0, 0.5, 2.0) & \text{if } x \geq 0.5\,. \end{cases}$$

This problem has a solution consisting of two strong rarefactions and a trivial stationary contact discontinuity. Figures 8 and 9 shows the solution profiles at $t = 0.5$. We use 400 mesh points in the spatial domain. In the figures we can see a downward peak at the middle of the contact discontinuity in the Godunov solution. This type of intability usually happens in the Godunov scheme as discussed in the intrdoduction.

Problem 4: Perturbed relativistic shock tubbe flow

The initial conditions are specified as $(n_L, u_L, p_L) = (1.0, 0.0, 1.0)$ for $0 \leq x \leq 0.5$ and $(n_R, u_R, p_R) = (n_R, 0.0, 0.1)$ for $0.5 \leq x \leq 1.0$. Here the right state is a purturbed density field of sinusoidal wave, $n_R = 0.125 - 0.0875\ \sin(50(x - 0.5))$. We run this test for the 400 mesh points. The computed solutions are plotted at $t = 0.5$. The results are shown in Figure 10. Since the continuity equation in the Euler equations decouples from the other two equations for the pressure and velocity, therefore we do not see the effect of perturbation in the pressure.

Problem 5: Two Interacting Relativistic Blast Waves

We consider here the interaction of two relativistic blast waves. The intial data are

$$(n, u, p) = \begin{cases} (1.0, 0.0, 100.0) & \text{if } 0 < x < 0.1\,, \\ (1.0, 0.0, 0.06) & \text{if } 0.1 < x < 0.9\,, \\ (1.0, 0.0, 10.0) & \text{if } 0.9 < x < 1.0\,. \end{cases}$$

The reflective boundary conditions are applied at both $x = 0.0$ and $x = 1.0$. The results are given in Figure 11 for the particle density n, velocity $v = \frac{u}{\sqrt{1+u^2}}$ and pressure p. The number of mesh points are 700 and the output time is $t = 0.75$.

Problem 6: Implosion in a box.

In this example we consider a two-dimensional Riemann problem inside a square box of sides length 2, with reflecting walls. Initially the velocities are zero. The pressure is 10 and density is 4 inside a small square box of sides length 0.5 in the center of the large box, while pressure and density are unity elsewhere. The results are shown at $t = 3.0$ in Figures 12, 13, while at $t = 12.0$ in Figures 14 and 15. In all the results we have used 400×400 mesh points.

Problem 7: Cylindrical Explosion Problem.

Consider a square domain $[0, 2] \times [0, 2]$. The initial data are constant in two regions separated by a circle of radius 0.4 centered at $(1, 1)$. Inside the circle density is 5.0 and the pressure is 10.0 , while outside the density is 1.0 and pressure is equal to 0.5. The velocities are zero everywhere. The solution consits of a circular shock wave propagating outwards from the origin, followed by a circular contact discontinuity propagating in the same direction, and a circular rarefaction wave travelling towards the origin. The results ar shown in Figure 16 and Figure 17 for 400×400 mesh points at $t = 0.4$.

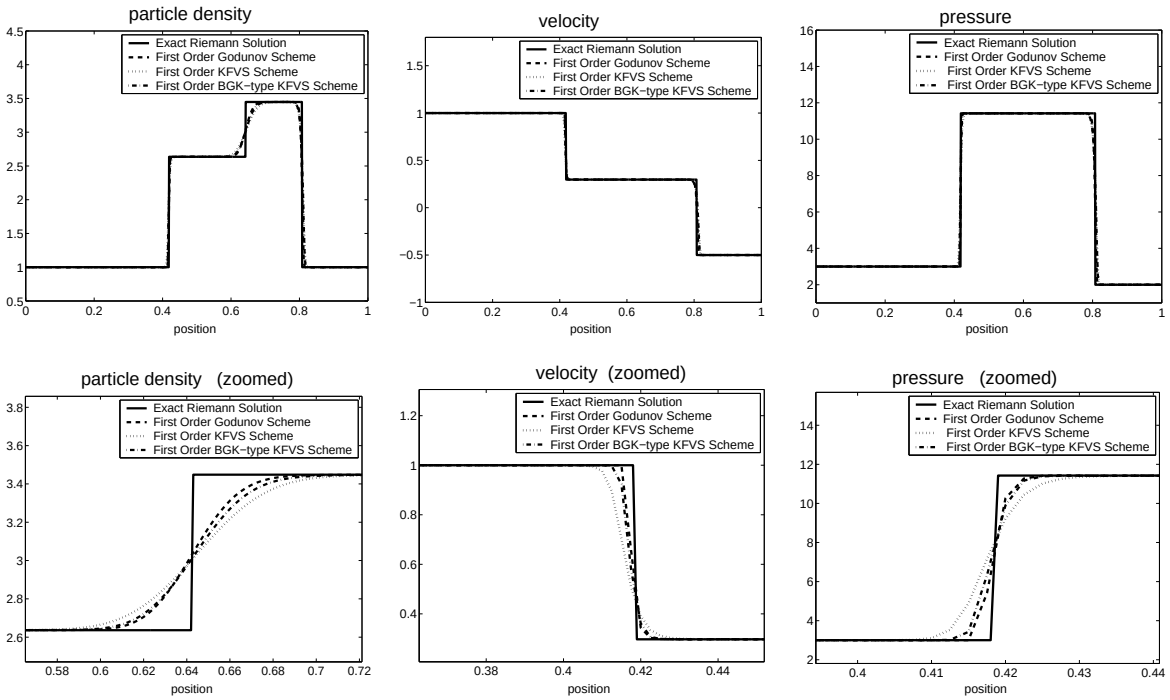

Figure 4: Comparison of the first order schemes at $t = 0.5$.

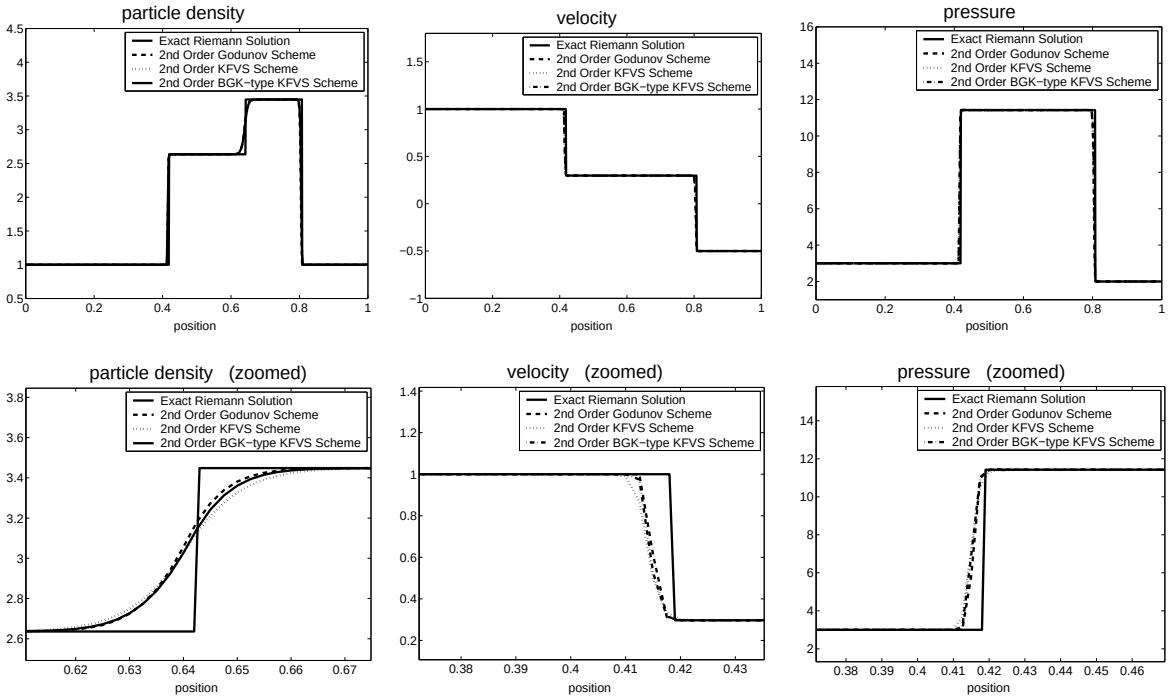

Figure 5: Comparison of the 2nd order schemes at $t = 0.5$.

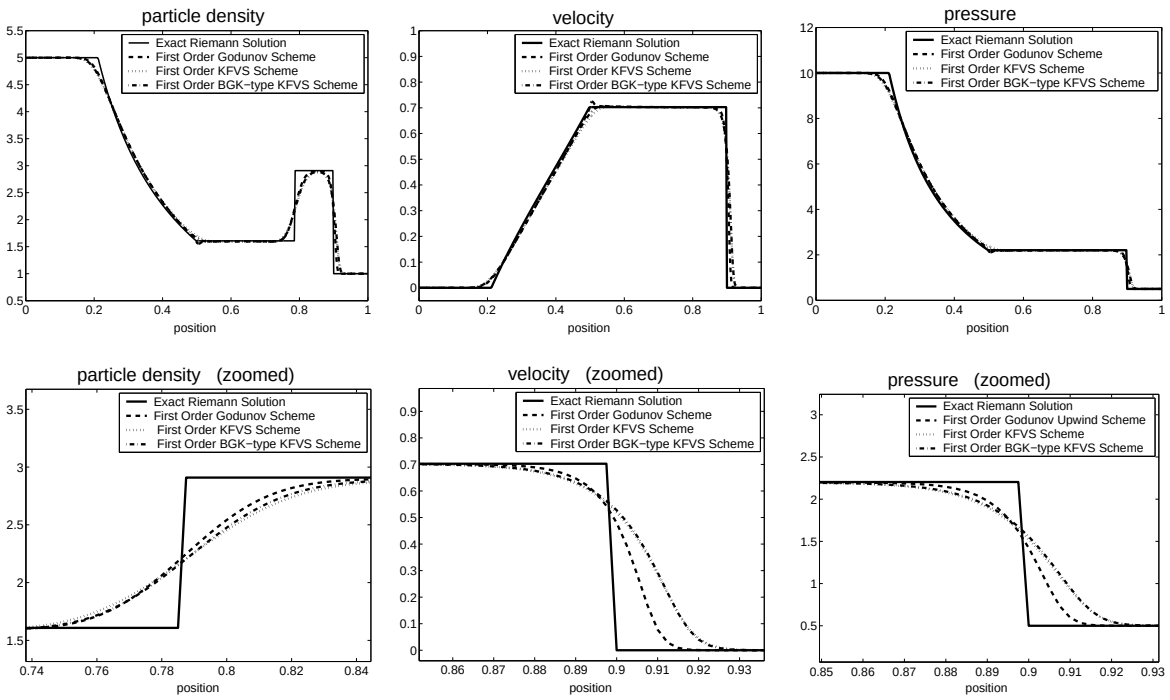

Figure 6: Comparison of the first order schemes at $t = 0.5$.

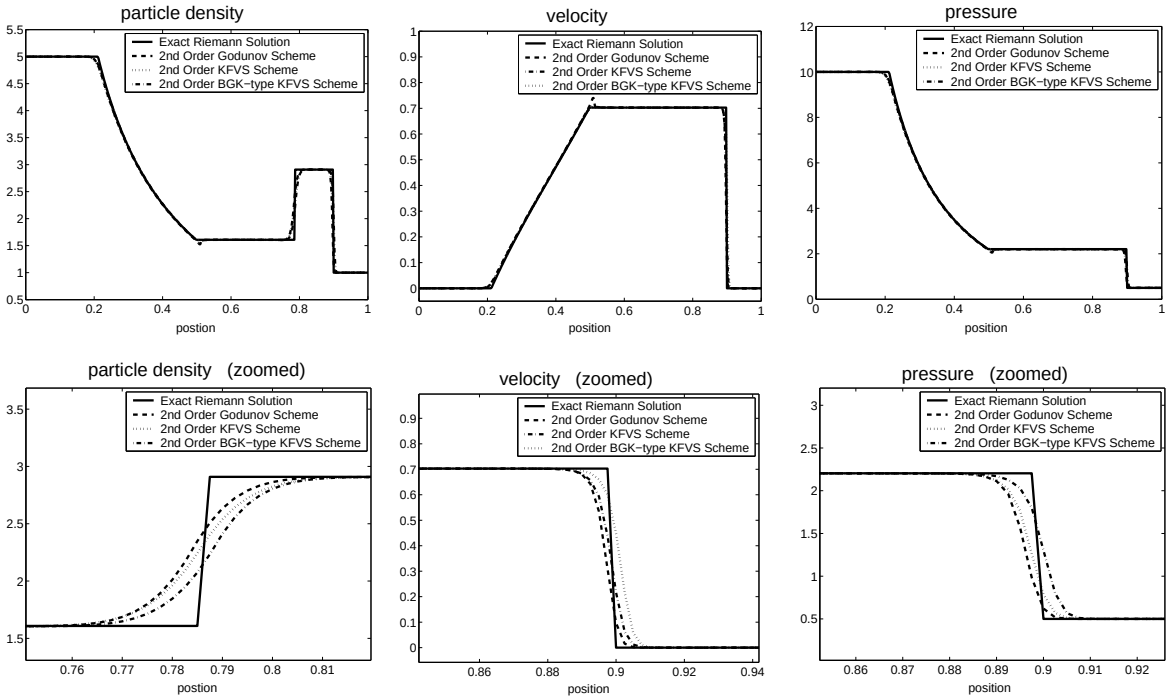

Figure 7: Comparison of the 2nd order schemes at $t = 0.5$.

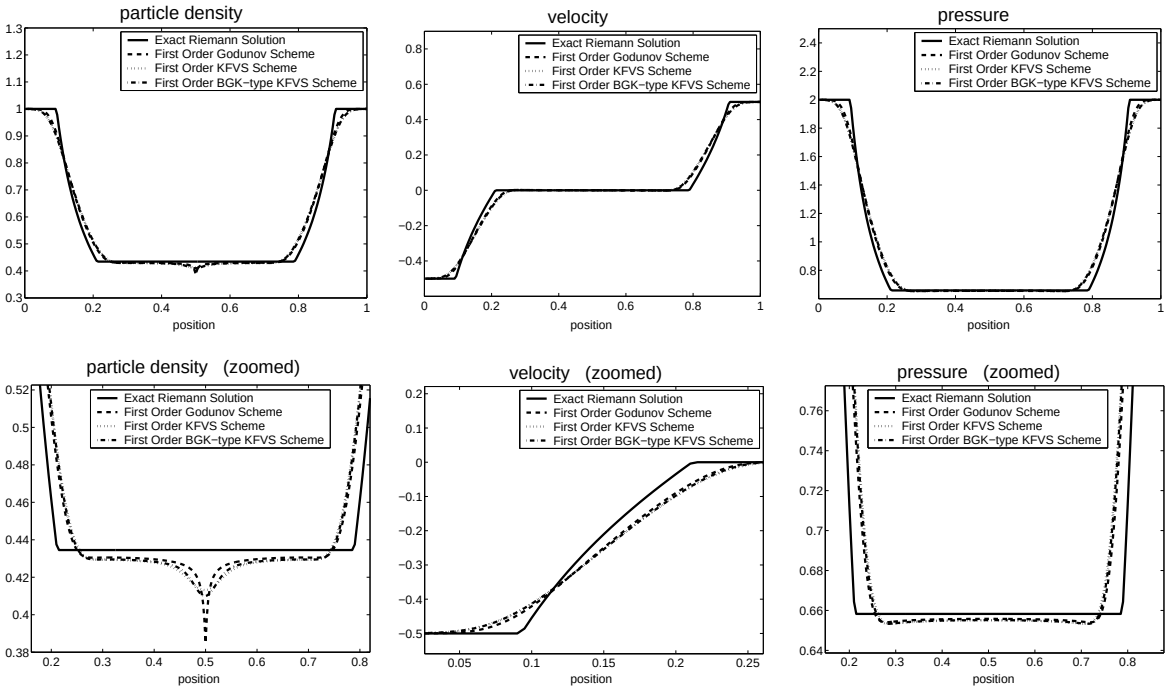

Figure 8: Comparison of the first order schemes at $t = 0.5$.

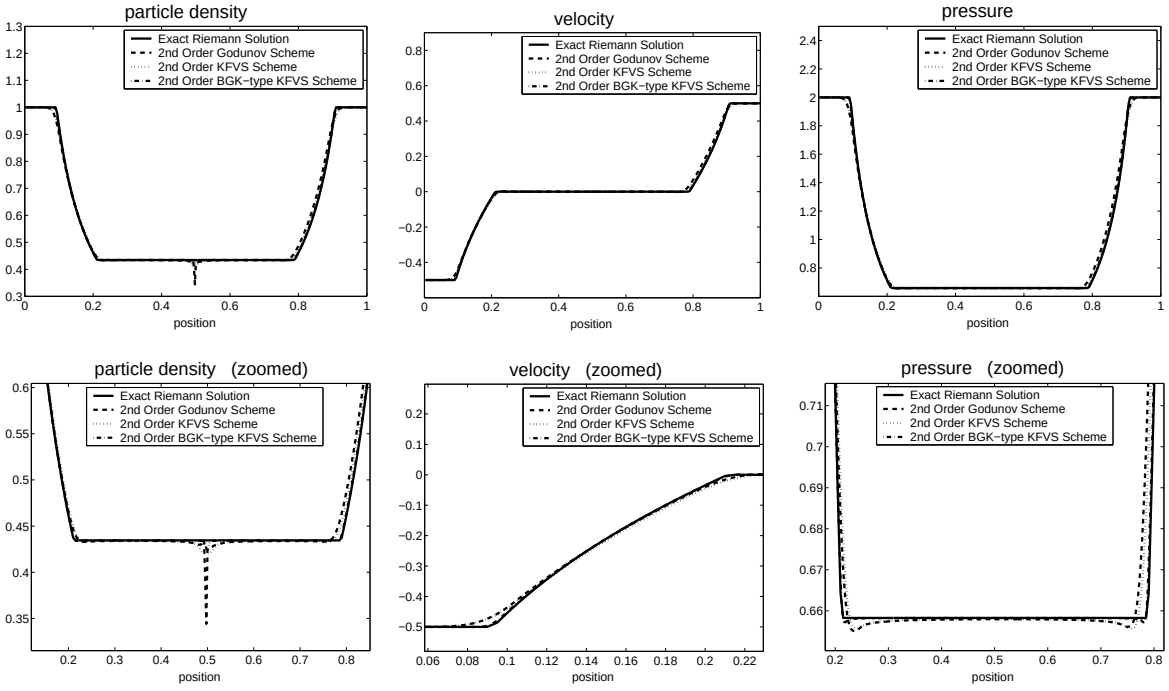

Figure 9: Comparison of the 2nd order schemes at $t = 0.5$.

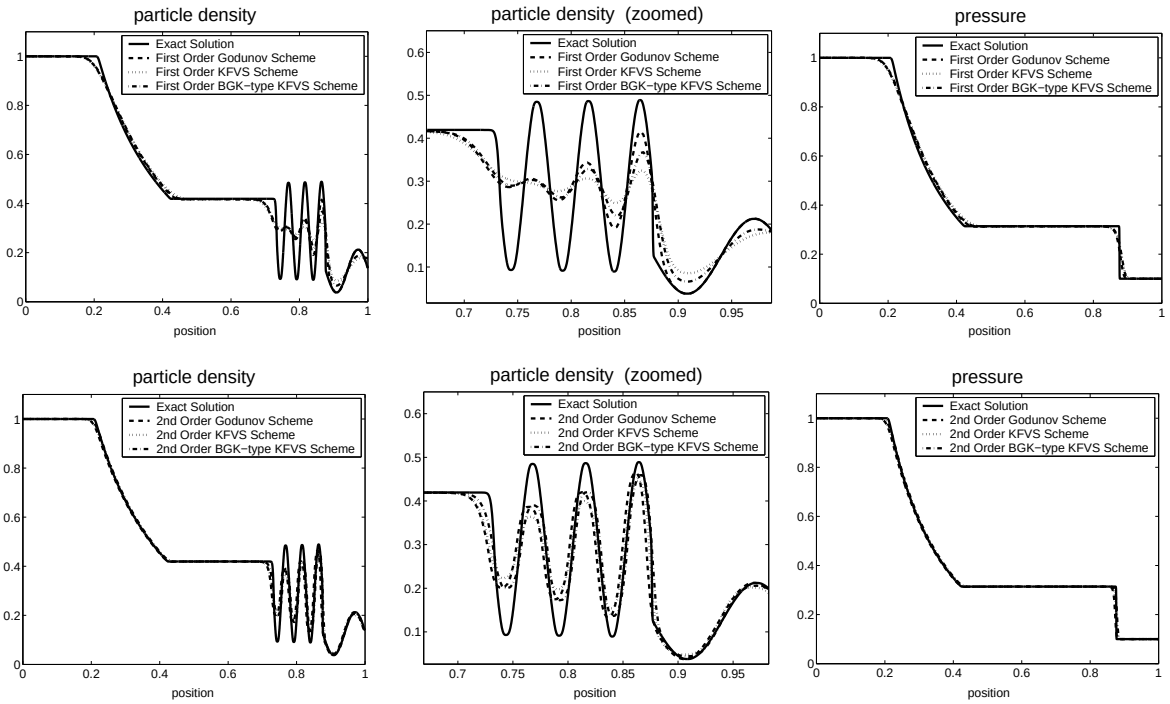

Figure 10: Purturbed relativistic shock tube flow at time $t = 0.5$.

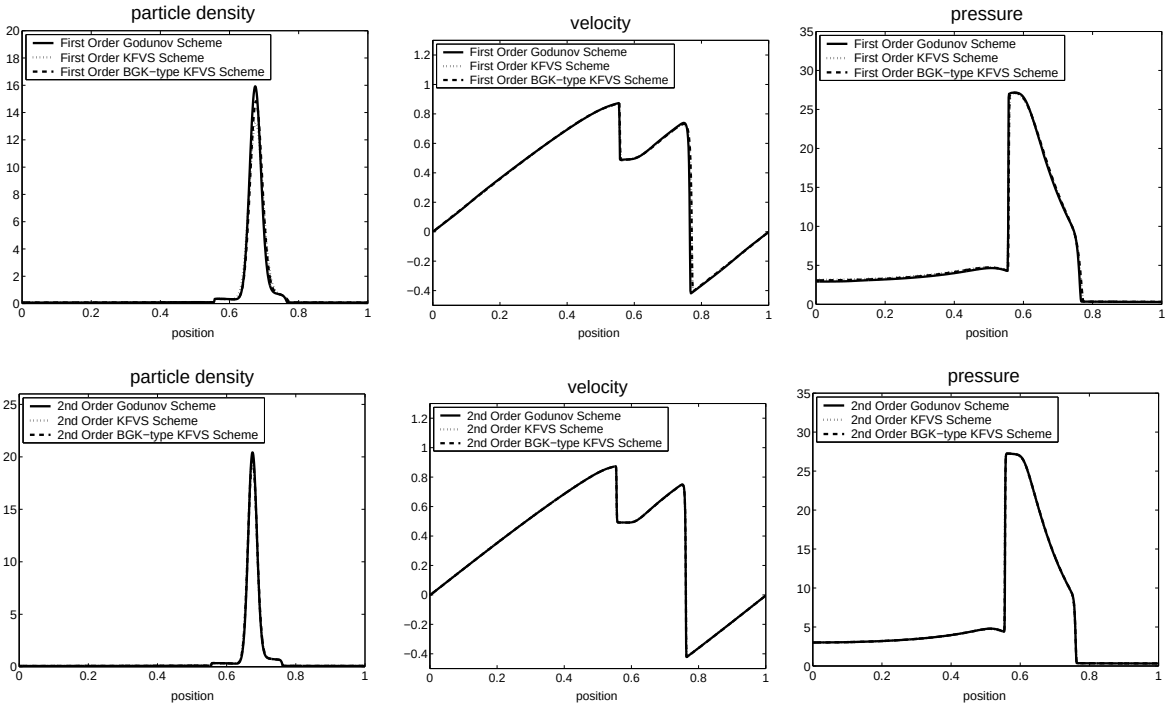

Figure 11: Two interacting relativistic blast waves at time $t = 0.75$.

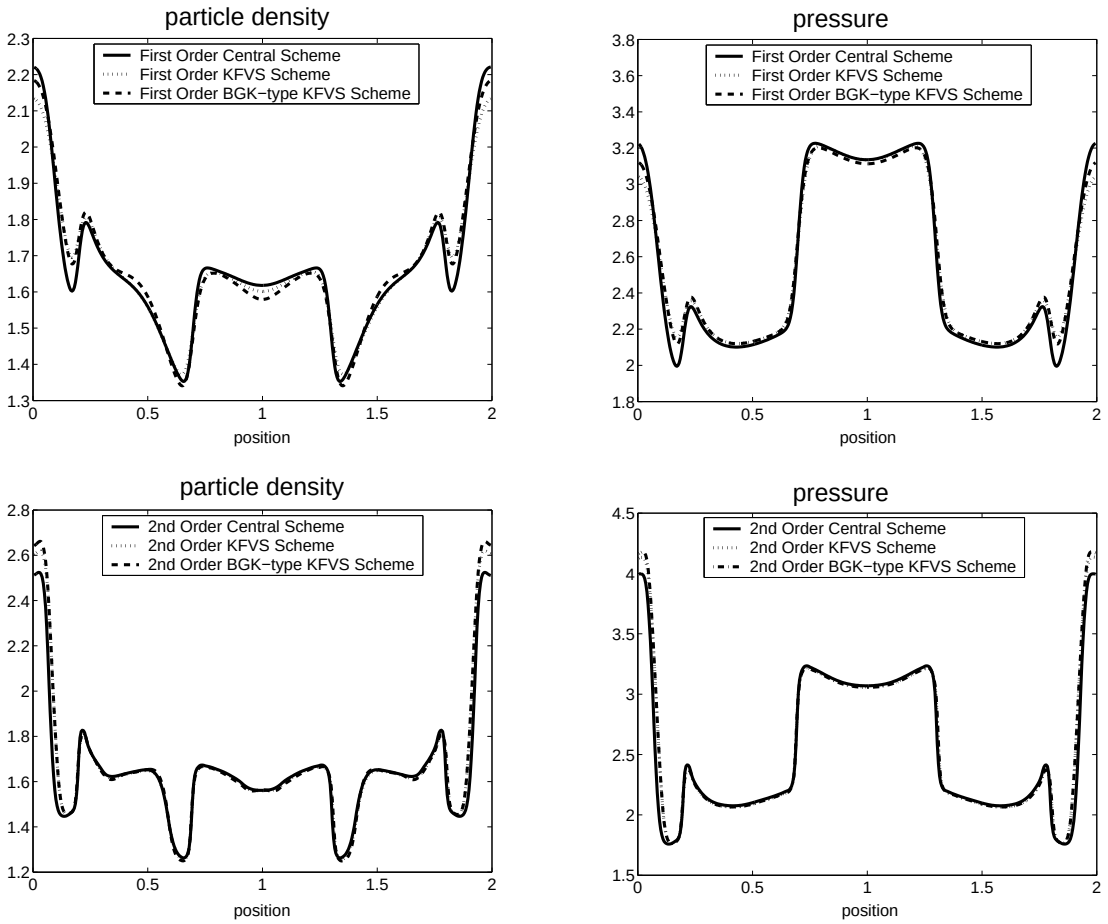

Figure 12: First and second order schemes for the implosion in a box at $t = 3.0$.

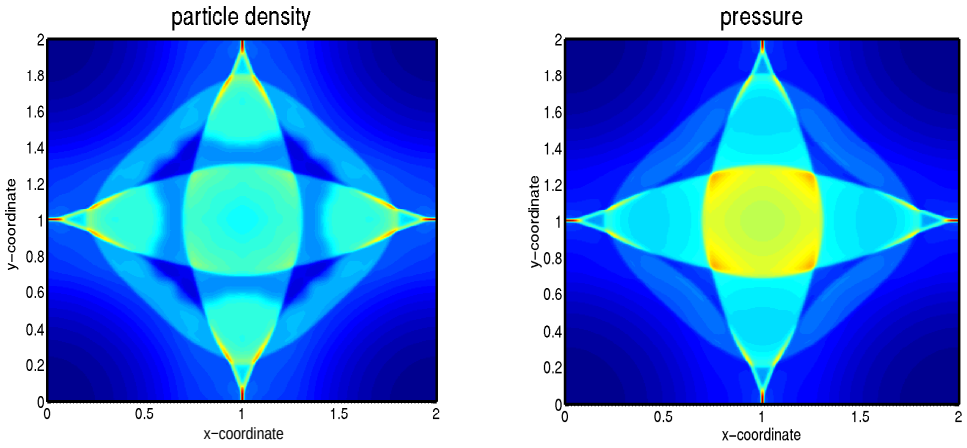

Figure 13: BGK-type KFVS scheme applied to implosion in a box at $t = 3.0$.

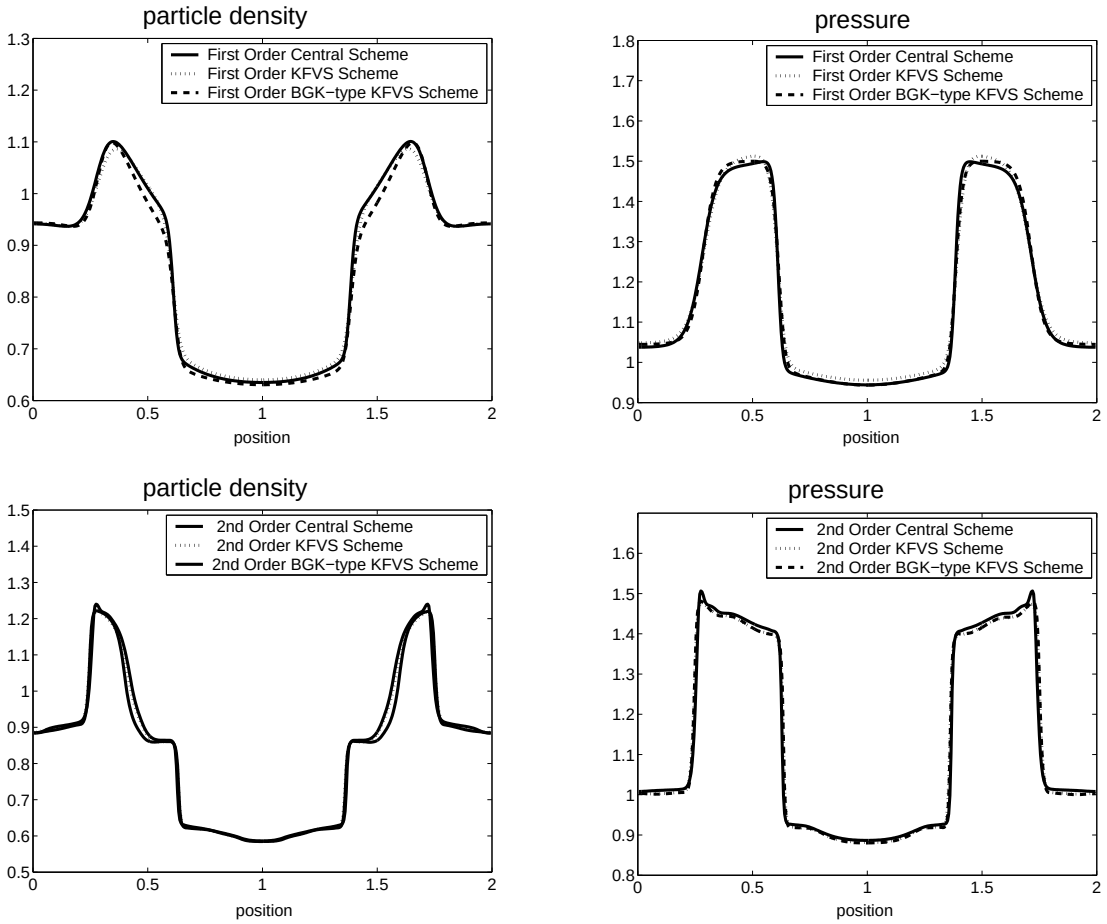

Figure 14: First and second order schemes for the implosion in a box at $t = 12.0$.

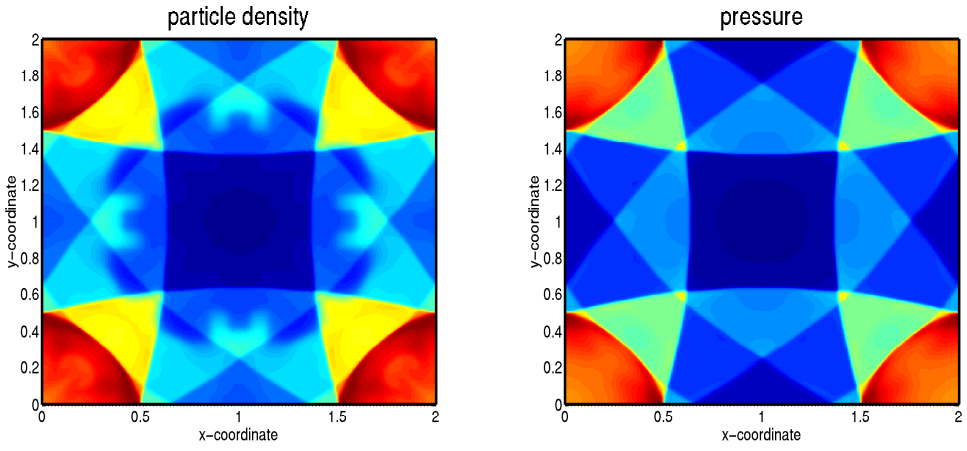

Figure 15: BGK-type KFVS scheme for the implosion in a box at $t = 12.0$

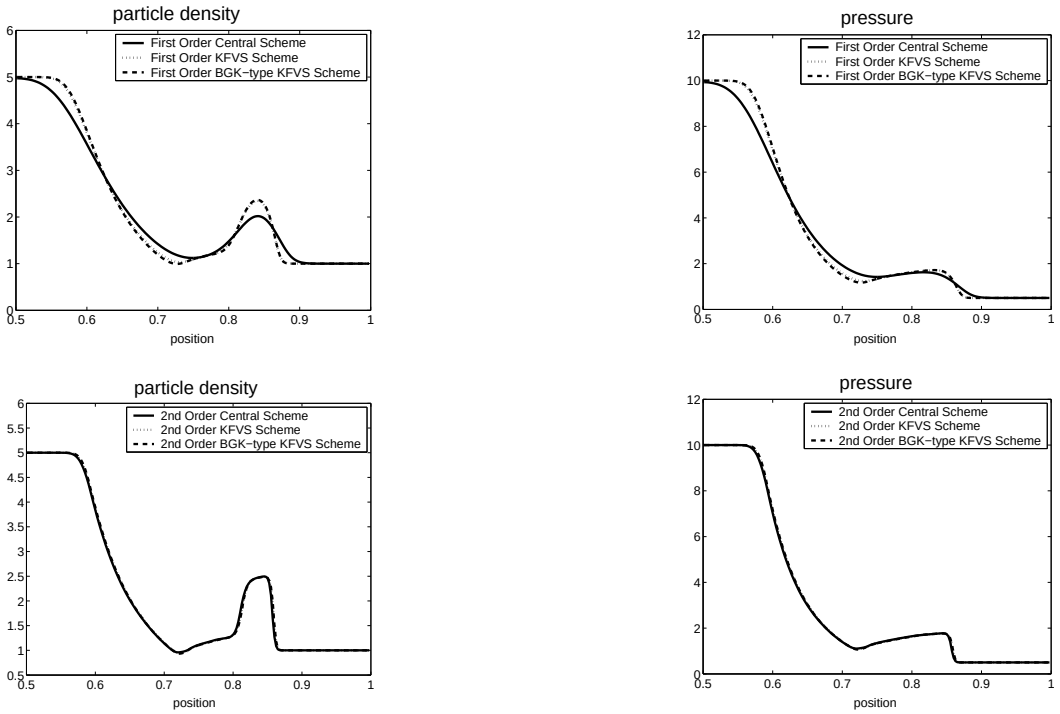

Figure 16: Comparison of the schemes applied to cylinderical explosion at $t = 0.2$.

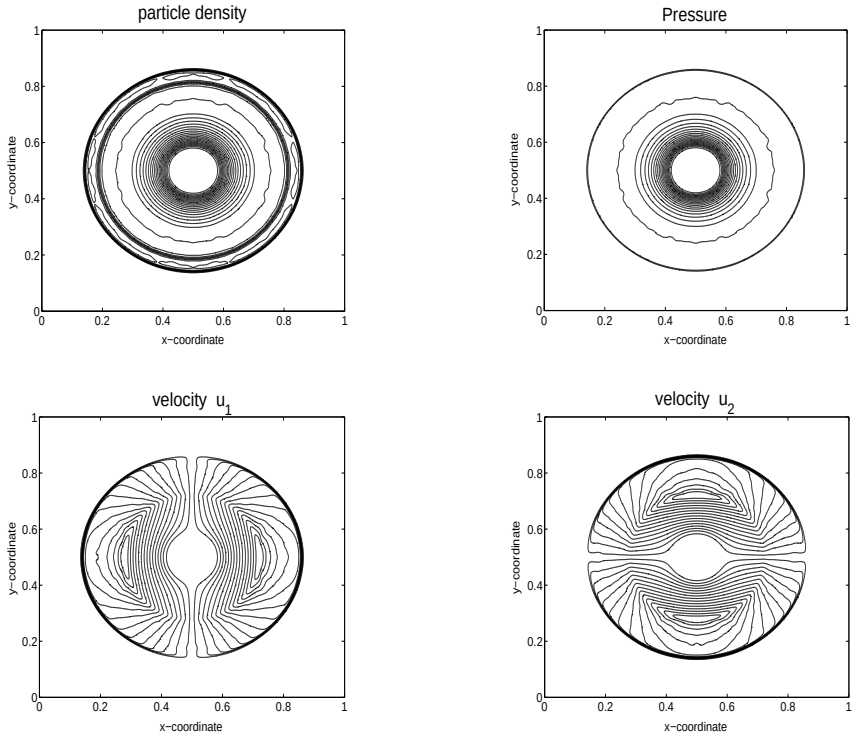

Figure 17: BGK-type KFVS scheme applied to cylinderical explosion at $t = 0.2$.

References

[1] P.L. Bhatnagar, E.P. Gross, M. Krook, "A model for collision processes in gases", *Acta Phys.,* **23**, (1964). *Phys. Rev.* 94 (1954) pp. 511.

[2] C. Cercignani, "The Boltzmann equation and its applications", *Applied Mathematical Sciences* **67**, Springer Verlag, New York (1988).

[3] S. M. Deshpande, "A second order accurate, kinetic-theory based, method for inviscid compressible flows", NASA Langley Tech. paper No. 2613, (1986).

[4] S. M. Deshpande, S. Sekar, S. Nagaratinam, M. Krishnamurthy, R. Sinha and P.S. Kulkarni, "A 3-dimensional upwind Euler solver using kinetic flux vector splitting method", *In the 3rd International Conference on Numerical Methods in Fluid Dynamics*, Lecture Notes in Physics, Springer-Verlag **414** (1992) pp. 105-109.

[5] S. M. Deshpande and P.S. Kulkarni "New developments in kinetic schemes", *Computer math. Applic.*, **35**, (1998) pp. 75-93.

[6] S. M. Deshpande, "Kinetic flux splitting schemes", *In Computational Fluid Dynamics Review 1995, (Edited by M. Hafez and K. Oshima)*, John Wiley & Sons, (1995).

[7] W. Dreyer and M. Kunik, "The maximum entropy principle revisited", *Cont. Mech. Thermodyn.* **10** (1998) pp. 331-347.

[8] B. Enfield, C.D. Munz, P.L. Roe and B. Djogreen "On Godunov type methods near low density", *J. Comput. Phys.*, **92**, (1991) pp. 3273-295.

[9] E. Godlewski and P.A. Raviart, "Numerical approximation of hyperbolic systems of conservation laws", *Springer*, (1996).

[10] S.K. Godunov "A difference scheme for numerical computation of discontinuous solution of hydrodynamic equations", *Math. Sbornik*, **47**, 271 (1959).

[11] S.R. deGroot, W.A. van Leeuven and Ch.G. van Weert, "Relativistic kinetic theory. Principles and Applications", North Holland, Amsterdam (1980).

[12] A. Harten, P.D. Lax and B. van Leer "On upstream differencing and Godunov-type schemes for hyperbolic conservation laws", *SIAM Review*, **25**, (1983) pp. 35-61.

[13] J.F. Hawley, L.L. Smarr, J.R. Wilson, "A Numerical Study of Nonspherical Balck Hole Accretion. I. Equations and Test Problems", *The Astrophysical Journal* **277**, (1984) pp. 296-311.

[14] F. Jüttner, "Das Maxwellsche Gesetz der Geschwindigkeitsverteilung in der Relativtheorie", *Ann. Phys.* (Leipzig), **34**, (1911) pp. 856-882.

[15] F. Jüttner, "Die Relativistische Quantentheorie des idealen Gases", *Z. Phys.* **47**, (1928) pp. 542-566.

[16] M. Kunik, S. Qamar and G. Warnecke, "Kinetic schemes for the ultra-relativistic Euler equations", Preprint Nr. **21**, Otto-von-Guericke University, (2001).

[17] M. Kunik, S. Qamar and G. Warnecke, "Kinetic schemes for the relativistic gas dynamics", Preprint Nr. **21**, Otto-von-Guericke University, (2002).

[18] B. van Leer, "Toward the ultimate conservative difference schemes V: A second order sequel to Godunov's method", *J. Comput. Phys.*, **32** (1979) 101-136.

[19] B. van Leer, "Flux vector splitting for the Euler equations", ICASE Report No. 82-30 (1982).

[20] S. Lui and K. Xu, "Entropy analysis of kinetic flux vector splitting scheme for the compressible Euler equations", NASA/CR-1999-208981, ICASE Report No. 99-5, (1999).

[21] J.C. Mandal and S.M. Deshpande, "Kinetic flux -vector splitting for Euler equations", *Computer & Fluids,* **23**(**2**), (1994) pp. 447-478.

[22] J.Mª Martí, E. Müller, "Numerical Hydrodynamics in Speical Relativity", *Living Reviews in Relativity* **2** (1999) p. 1-101.

[23] J.V. Neumann and R.D Richtmyer , *Appl. Phys.,* **21**, 232, (1950).

[24] S. Osher and F. Solomon, "Upwind difference schemes for hyperbolic systems of conservation laws", *Math. Comput.,* **38** (1982), pp. 339-374.

[25] B. Perthame, "Second-Order Boltzmann Scheme for Compressible Euler Equations in One and Two Space Dimensions", *SIAM J.Numer.Anal.* **29, No.1** (1992), pp. 1-19.

[26] D.I.Pullin, "Direct simulations methods for compressible inviscid ideal gas-flows", *J. Comput. Phys.* **34, No. 1** (1980), pp. 231-244.

[27] Quirk, J., "A contribution to the great Riemann solver debate", *Int. J. Num. Met. in Fluids* **18, No. 6** (1994).

[28] P.L. Roe, "Approximate Riemann Solvers, parameter vectors and difference scheme", *J. Comput. Phys.* **43,** 357 (1981).

[29] J. L. Steger and R.F Warming, "Flux vector splitting of the inviscid gas dynamic equations with applications to finite difference methods", *J. Comput. Phys.* **40,** (1981), pp. 263-293.

[30] T. Tang and K. Xu, "Gas-kinetic schemes for the compressible Euler Equations I: positivity-preserving analysis", To appear in ZAMP (1998).

[31] E.F. Toro, "Riemann solvers and numerical method for fluid dynamics", Second Edition, Springer-Verlag, (1999).

[32] G. Toth and D. Odstrcil"Comparison of some flux corrected transport and total variation diminishing numerical schemes for hydrodynamic and magnetohydrodynamic problems ", *J. Comput. Phys.*,**128**, (1996) pp. 82-100. *J. Comput. Phys.*

[33] N.P. Weatherill, J.S. Mathur and M.J. Marchant, "An upwind kinetic flux vector splitting method on general mesh topologies", *International Journal for Numerical Methods in Engineering*, **37**(**2**), (1994) pp. 623-643.

[34] S. Weinberg, "Gravitation and Cosmology", Wiley, New York, (1972).

[35] K. Xu, L. Martinelli and A. Jameson, "Gas-kinetic finite volume methods, flux-vector splitting and artificial diffusion ", *J. Compute. Phys.*, **120** (1995), pp. 48-65.

[36] K. Xu, "Gas kinetic schemes for unsteady compressible low simulations", 29th CFD, Lecture Series (1998).

[37] K. Xu, "Gas-kinetic theory based flux slitting method for ideal magnetohydrodynamics", ICASE Report No. Tr. 98-53, (1998).

[38] K. Xu, "Gas evolution dynamics in Godunov-type schemes and analysis of numerical shock instability", ICASE Report No. Tr. 99-6, (1998).